THE ACOUSTIC WAVE PROPAGATION EQUATION: THE DISCONTINUOUS GALERKIN TIME DOMAIN SOLUTION APPROACH

BY

KOECH PRISCA CHEPKURUI

A THESIS SUBMITTED IN PARTIAL FULFILMENT OF THE REQUIREMENTS FOR THE DEGREE OF MASTER OF PHILOSOPHY IN APPLIED MATHEMATICS IN THE DEPARTMENT OF MATHEMATICS AND COMPUTER SCIENCE OF UNIVERSITY OF ELDORET, KENYA

MAY, 2019

DECLARATION

Declaration by the Candidate

This thesis is my original work and has not been presented for award of a degree in any other University. No part of this thesis may be reproduced without the prior written permission of the author and/or University of Eldoret.

KOECH PRISCA CHEPKURUI

SC/PGM/04/06 **Signature..... Date.....**

Declaration by Supervisors

This thesis has been submitted for examination with our approval as the university supervisors;

Prof. Alfred W. Manyonge

Department of Pure and Applied Mathematics,

Maseno University,

P.O. Box 333-40105, Maseno, Kenya.

Signature..... Date.....

Prof. Jacob K. Bitok

Department of Mathematics and Computer Science,

University of Eldoret

P.O. Box 1125-30100, Eldoret, Kenya.

Signature..... Date.....

DEDICATION

This thesis is dedicated to my beloved dad James Koech and mum Martha Koech for their constant moral support and prayers through the period of my research. I also dedicate this work to my beloved husband Jared Mbera for his financial support and my dear children Roy Miyogo, Ray Kiplagat, Reu Omari, and Rehema Kemunto for their constant encouragement during the study period.

ABSTRACT

This thesis presents a finite element method, discontinuous Galerkin time domain approach that solves the 2-D acoustic wave equation in cylindrical coordinates. The method is based on discretization of the wave field into a grid of (r,θ) where r is the distance from the centre and θ is the radial angle. The Galerkin formulation is used to approximate the solution of the acoustic wave equation along the r coordinate and θ coordinate derivatives. The boundary conditions applied at the boundaries of the numerical grid are the free surface boundary condition at $r = 1$ and the absorbing boundary condition applied at the edges of the grid at $r = 2$. The solution is based on considering wave motion in the direction normal to the boundary, which in this case is the radial direction over radial angle $\theta \in [0^o, 30^o]$. The exact solution is described in terms of Bessel function of the first kind, which forms the basis of the boundary conditions for the values of pressure and eventually sufficient accuracy of the numerical solution. The obtained Matlab algorithm is tested against the known analytical solution, which demonstrates that, pressure of the wave increases as the radius increases within the same radial angle. The domain was discretized using linear triangular elements. The main advantage of this method is the ability to accurately represent the wave propagation in the free surface boundary with absorbing boundary condition at the edges of the grid, hence the method can very accurately handle wave propagation on the surface of a cylindrical domain. The resulting numerical algorithm enables the evaluation of the effects of cavities on seismograms recorded in boreholes or in cylindrical shaped tunnels.

TABLE OF CONTENTS

LIST OF FIGURES

LIST OF TABLES

SYMBOLS AND NOTATIONS

$c - wave\ speed.$

$k - wave\ number$

$\beta - Bulk\ modulus$

$p - acoustic\ pressure$

$\rho - density\ of\ the\ fluid$

$t - time$

$\Gamma - free\ surface$

$\Omega - domain$

$f - frequency$

$u - particle\ velocity$

$A - amplitude$

$\omega - angular\ frequency$

DG- Discontinuous Galerkin

FD- Finite Difference

DGTD- Discontinuous Galerkin Time-Domain

1D- One dimension

2D- Two Dimensions

P.D.E- Partial Differential Equation

$L - differential\ operator$

$i, j, k - integers$

$m - number\ of\ elements$

$N - number\ of\ finite\ elments$

$\phi - shape\ (basis) functions$

$n - unit\ outward\ normal$

$q - number\ of\ unknown\ nodal\ quantities$

$b - vector$

r - radius

θ - radial angle

ACKNOWLEDGMENT

I am profoundly grateful to my research supervisor Prof. Alfred Manyonge and Prof. Jacob Bitok for their guidance into the research problem and timely relentless encouragement throughout the undertaking of the work.

I would also like to specifically thank Mr Albert Bii for his guidance and support in providing helpful discussions to the success of the thesis.

My special thanks also go to all members, students and lecturers of the mathematics department for their advice and cooperation which made it possible to accomplish this task on time.

I am also very grateful to God Almighty for His protection and all Providences throughout the research.

Finally, my very special thanks to my family members for their patience and support throughout the research.

CHAPTER ONE

INTRODUCTION

Acoustic or Sound wave propagation is motion of sound waves in heterogeneous media (fluids and solids). There are numerous numerical methods for solving different types of partial differential equations that describes the physical dynamics of the world for instance PDE's are used to understand fluid flow for aerodynamics, wave dynamics for seismic exploration and orbital mechanics. For many seismic processing procedures, the numerical modeling of seismic waves is an essential part of the process. When attempting to image the subsurface of the earth based on the difference between the response of the modeled system, it is sometimes necessary to iteratively update the current model and the data recorded from the actual experiment. Therefore it is important that both the numerical method and the type of model used in the forward modeling, are capable of accurately representing the physical experiment, this is according to Matt et al (2012). A specific type of numerical method is required in solving partial differential equations that accurately model the earth's properties. More precisely, because of the discontinuous nature of the earth's properties, the PDE's exhibit a low-order level of continuity at the discontinuous interfaces. Approximation methods that assume a higher level of continuity, can cause the position of these kinks to show up at incorrect spatial locations, leading to improperly reconstructed earth models according to Matt et al (2012). This thesis begins with the formulation of the acoustic wave propagation equation in the fluid medium. We also highlight some of the numerical methods used to solve PDE's and discuss the necessary concepts to understand Discontinuous Galerkin. The Galerkin formulation solves the weak form of the PDE representing wave propagation and naturally includes boundary integral terms to represent free surface, rigid and absorbing

boundary effects. These concepts are then used in formulating DG for 2D acoustic wave equation under uniquely formulated boundary conditions and its solution compared to the exact solution in terms of convergence and accuracy. The Matlab code is used to compute the results of the acoustic wave problem.

1.1 Background of the Problem

Sound is a wave phenomenon by which energy is transmitted through a medium via fluctuations in pressure and fluid vibration. To illustrate the physical process of the acoustic waves, a fluid (a gas or a liquid) is enclosed in a semi-infinite tube with a sliding piston at one end. It is assumed that the tube is sufficiently narrow for all variations in fluid properties to depend only on the axial coordinate x. However, the influence of the walls is neglected. In a narrow tube, viscous effects lead to energy loss in the vicinity of the walls but this is neglected here. Such one-dimensional waves are called plane waves, as the acoustic fluctuations are uniform on any plane perpendicular to the axial direction. (Frank and David (2015)). The compressibility of the fluid plays a central role in the propagation of acoustic disturbances. If the fluid in the tube were incompressible and did not deform at all, then all of the fluid in the tube would move at the same instant as the piston. However, if the fluid is compressible and has inertia, it takes a finite time for the disturbance caused by the motion of the piston to be transmitted to the fluid. The speed at which this is transmitted is the speed of sound. In the physical process involved, first, the fluid immediately in front of the piston becomes compressed. The compression is then transmitted down the tube. The leading edge of the disturbance, having an increased pressure over the ambient pressure, moves at the speed c_0, the speed of sound. As the compression moves down the tube, more and more of the fluid reaches the velocity u at which the piston is

moving. If the piston is suddenly brought to rest, then the fluid immediately in front of the piston will also come to rest; nevertheless, both the leading and the trailing edges of the disturbance continue to propagate at the velocity c_0, and as the compression passes down the tube it imparts a velocity u to the fluid as it passes. This illustrates the important distinction between the velocity c_0 at which the compression propagates and the velocity u which the fluid reaches as the compression passes through a given local region of fluid. The latter is known as the particle velocity, which corresponds to the passage of an acoustic wave. (Frank and David (2015)).

Sound waves in a fluid (air or water) are longitudinal waves. The particles in the medium are displaced from their equilibrium position parallel to the direction that the wave propagates.

1.1.1 Wave propagation speed

The wave speed is determined by the properties of the medium. In general the speed of a mechanical wave depends on the resilience of the medium as well as its mass density. The more rigid the medium the faster the wave propagation speed. But the higher the mass density, the slower the wave speed. For sound waves through air or water, the wave speed would depend on the compressibility of the medium and the volume mass density. An example of wave motion involves a wave function that is sinusoidal (Herrin 2012). The disturbance is in the shape of a sine wave. The resulting wave motion description is then

$$u(x,t) = A\sin(kx \pm \omega t) \tag{1.1}$$

$k = wave\ number,\ \omega = angular\ frequency, A = amplitude$

The amplitude of the wave is the maximum displacement of any part of the medium from the equilibrium or undisturbed position. The frequency F, the period T of

oscillation, the wavelength λ, the wave number k, the wave speed c and the wave function $u(x,t)$ can be related in the form

$$u(x,t) = A\sin(kx \pm \omega t) = A\sin(\frac{2\pi}{\lambda}x \pm 2\pi Ft) = A\sin k(x \pm ct) \qquad (1.2)$$

1.1.2 Speed of Sound

The general principles in the discussions of wave motion apply equally to sound. The propagation of a disturbance in air is described by a differential equation of the same form as equation (1.1). So the solutions to the equation are necessarily of the form as equation (1.2). The wave speed c depends on the bulk modulus β and on the mass density ρ of the fluid.

$$c = \sqrt{\frac{\beta}{\rho}} \qquad (1.3)$$

The bulk modulus refers to how resistant the fluid is to a change in its volume and is given by

$$\beta = \frac{volume\ stess}{volume\ strain} = -\frac{\Delta P/_P}{\Delta V/_V}$$

with ΔP as the change in pressure P and ΔV as the change in volume V. For a sound wave in air $c = 340ms^{-1}$, For a sound in water $c = 1500ms^{-1}$

In the field of mechanical wave propagation, two wave types are distinguished depending on the properties of the underlying propagation medium. Traditionally, waves in fluids are called acoustic waves and waves in solids are known as elastic waves.

1.1.3 Derivation of 1-D Acoustic wave equation

To describe the propagation of acoustic disturbances in a fluid such as air or water, we first consider a one–dimensional situation before turning to a two-dimensional situation. Consider a tube of cross-sectional area S, containing air at ambient pressure p_0 and pressure which is the sum of ambient pressure and the acoustic pressure, $p_{tot} = p_0 + p$ where p is small compared to p_0. Similarly, as the fluid is compressed or rarefied, its density will vary from its nominal value ρ_0 and this can also be written as $\rho_{tot} = \rho_0 + \rho$, where ρ is the 'acoustic' fluctuation of the density, which is much smaller than ρ_0. The fluid also experiences motion within the tube which can be described by its particle velocity u in the x direction.

1.1.3.1 Equation of mass conservation

Consider a fluid volume of infinitesimal length δx and the mass of fluid within this volume is given by $\rho_{tot}\delta x S$. We are interested in the rate of increase of mass within the volume, which can be written as

$$\frac{\partial \rho_{tot}}{\partial t}\delta x S = \frac{\partial \rho}{\partial t}\delta x S \tag{1.4}$$

as ρ_0 is independent of time. This must equal the flow of mass into the control volume. At the left-hand end, the rate of flow of mass into the volume is given by $\rho_{tot} u S$ evaluated at x, while at the right-hand end, the corresponding rate of flow of mass out of the volume is $\rho_{tot} u S$ evaluated as $x + \delta x$. For any quantity h, to a first-order approximation

$$h(x + \delta x) \equiv h(x) + \frac{\partial h}{\partial x}\delta x S \tag{1.5}$$

thus the rate of mass inflow into the control volume is given by

$$\rho_{tot} uS - \left[\rho_{tot} u + \frac{\partial(\rho_{tot} u)}{\partial x}\delta x\right] S = -\frac{\partial(\rho_{tot} u)}{\partial x}\delta x S \tag{1.6}$$

Expanding the derivative,

$$\frac{\partial(\rho_{tot} u)}{\partial x} = u\frac{\partial \rho_{tot}}{\partial x} + \rho_{tot}\frac{\partial u}{\partial x} \tag{1.7}$$

Substituting $\rho_{tot} = \rho_0 + \rho$ and noting that $\partial\rho_0/\partial x = 0$

$$\frac{\partial(\rho_{tot} u)}{\partial x} = u\frac{\partial \rho}{\partial x} + (\rho_0 + \rho)\frac{\partial u}{\partial x} \tag{1.8}$$

However, for small amplitudes, the terms $u(\partial\rho/\partial x)$ and $\rho(\partial u/\partial x)$, which are the product of

two small quantities, can be neglected, leaving only $\rho_0(\partial u/\partial x)$ on the right-hand side. Substituting this into (equation (1.6)) and equating it with (equation (1.4)) yields

$$\frac{\partial \rho}{\partial x} + \rho_0\frac{\partial u}{\partial x} = 0 \tag{1.9}$$

which is known as the linearized equation of mass conservation because it contains terms which are linear functions of the fluctuating quantities.(Frank and David (2015))

1.1.3.2 Equation of momentum conservation

The second equation required can be found by applying the principle of momentum conservation to a fluid element; in this case, we will apply the principle to an element that moves with the fluid. The net force acting on the fluid element in the positive x-direction is given by the difference in p_{tot} at the two sides of the element multiplied by the area S,

$$p_{tot}S - \left(p_{tot} + \frac{\partial p_{tot}}{\partial x}\delta x\right)S = -\frac{\partial p_{tot}}{\partial x}\delta xS = -\frac{\partial p}{\partial x}\delta xS \tag{1.10}$$

The momentum conservation principle states that this net applied force must be balanced by the acceleration of the fluid element multiplied by its mass, $m = \rho_{tot}\delta xS \approx \rho_0\delta xS$ (Newton's second law). The acceleration of the moving fluid element is given by

$$\frac{Du}{Dt} = u\frac{\partial u}{\partial x} + \frac{\partial u}{\partial t} \tag{1.11}$$

Where D/Dt is the total convective derivative. However, the first term, which expresses the effect of convection of the fluid, is the product of small quantities and can be neglected, so that the mass times the acceleration of the fluid element is given by

$$\rho_0\frac{\partial u}{\partial t} + \frac{\partial p}{\partial x} = 0 \tag{1.12}$$

This relationship is known as the linearized equation of momentum conservation or Euler's equation.

To relate the pressure and density, we assume that the density change in the fluid is determined solely by the pressure change in the fluid and is not independent on the

temperature change. This is despite the fact that the temperature of the fluid will fluctuate slightly during the course of the compression and rarefaction. In a particular case of a perfect gas undergoing such an adiabatic compression, the relationship between the total pressure and total density is given by

$$p_{tot} = p_0 \left(\frac{\rho_{tot}}{\rho_0}\right)^{\gamma} \tag{1.13}$$

Where γ is the ratio of the specific heats of the gas, which for air has the value 1.4.

The relation between the acoustic pressure and density can be found from the gradient of (equation (1.13)) evaluated at density ρ_0. This can be written as

$$\frac{p}{\rho} = \frac{\partial p_{tot}}{\partial \rho_{tot}}\Big]_{\rho_{tot}=\rho_0} = \gamma p_0 \frac{(\rho_{tot})^{\gamma-1}}{(\rho_0)^{\gamma}}\Big]_{\rho_{tot}=\rho_0} = \frac{\gamma p_0}{\rho_0} \tag{1.14}$$

1.1.3.3 The acoustic wave equation.

With differentiation of (equation 1.9) with respect to t and (equation 1,12) with respect to x, then eliminating the common term $\rho_0 \partial^2 u/\partial x \partial t$ gives

$$\frac{\partial^2 p}{\partial x^2} - \frac{\partial^2 \rho}{\partial t^2} = 0 \tag{1.15}$$

The acoustic pressure and density fluctuations are related by (equation 1.14). Substituting this into (equation 1.15) yields the one-dimensional wave equation in terms of acoustic pressure fluctuations.

$$\frac{\partial^2 p}{\partial x^2} - \frac{1}{c_0^2}\frac{\partial^2 p}{\partial t^2} = 0 \tag{1.16}$$

Where c_0 is given by

$$c_0^2 = \frac{\gamma p_0}{\rho_0} \tag{1.17}$$

c_0 is the speed at which acoustic disturbances travel in the medium. Note from (equation 1.14), that

$$p = c_0^2 \rho \tag{1.18}$$

in all linear acoustic fields, so that the density also satisfies the wave equation (as c_0 is a constant for a given medium), as does the particle velocity.

It also follows from the ideal gas equation, $p_{tot} = \rho_{tot} R T_a$, where R is the specific gas constant and T_a is absolute temperature (in Kelvin), that

$$c_0^2 = \gamma R T_a \tag{1.19}$$

(Equation 1.16) relates the way in which the acoustic pressure fluctuation behave with respect to space (as a function of the coordinate distance x) and with respect to time t. (Frank and David 2015)

1.1.4 Solutions of the one-dimensional wave equation

A general form of solution to equation (1.16) was given by d'Alembert;

$$p(x,t) = f(t - x/c) + g(t + x/c) \tag{1.20}$$

Where $f \; and \; g$ are arbitrary functions. The fact that these are solutions which can be readily demonstrated by differentiating the functions f and g. Thus for f:

$$\frac{\partial^2}{\partial t^2}\{f(t - x/c\} = f''(t - x/c) \tag{1.21}$$

Where the dash indicates the derivative of the function, and

$$\frac{\partial^2}{\partial x^2}\{f(t - x/c)\} = \frac{1}{c^2} f''(t - x/c) \tag{1.22}$$

Which indeed satisfy (equation 1.16). The same applies to g. The two functions also have a well-defined physical interpretation. The first function $f(t - x/c)$ describes pressure disturbance which is travelling in the positive x-direction. Conversely, the function

$g(t + x/c)$ describes a fluctuation which travels in the negative x-direction.

The functions f and g are harmonic in time. Using complex notation for a time-dependence $e^{i\omega t}$, the corresponding function f is given by

$$f(t - x/c) = Re\{Ae^{i\omega(t-x/c)}\} = Re\{Ae^{i(\omega t - kx)}\} \quad (1.23)$$

or, writing $A = ae^{i\varphi}$:

$$f(t - x/c) = \text{acos}(\omega t - kx + \varphi) \quad (1.24)$$

The quantity $k = \omega/c$ is known as the wavenumber, and can be seen to correspond to the phase change per unit distance, having units of radians per meter. It can be thought of as a spatial frequency. (Frank and David 2015).

1.1.5 Derivation of Two-Dimensional Acoustic wave equation

A two-dimensional acoustic wave equation can be found using Euler's equation and the equation of continuity. (Ahmad 2000).

$$\frac{\partial p}{\partial t} + \rho c^2 \nabla . u = 0 \qquad \text{Continuity} \quad (1.25)$$

$$\frac{\partial u}{\partial t} + \frac{1}{\rho}\nabla p = 0 \qquad \text{Euler} \quad (1.26)$$

where u is the particle velocity, p is the acoustic pressure, $\rho = \rho(x, z)$ is the density and $c = c(x, z)$ is the velocity of the acoustic wave in the acoustic media. Substitution

of the divergence of the Euler's equation and the time derivative of the equation of continuity yield,

$$\frac{\partial^2 p}{\partial t^2} + \rho c^2 \left\{ -\nabla \left[\frac{1}{\rho} \nabla p \right] \right\} = 0 \tag{1.27}$$

$$\frac{\partial^2 p}{\partial t^2} - \rho c^2 \left\{ \frac{\partial}{\partial x} \left(\frac{1}{\rho} \frac{\partial p}{\partial x} \right) + \frac{\partial}{\partial z} \left(\frac{1}{\rho} \frac{\partial p}{\partial z} \right) \right\} = 0 \tag{1.28}$$

which is then simplified as follows:

$$\frac{\partial^2 p}{\partial t^2} - c^2 \left\{ \frac{\partial^2 p}{\partial x^2} + \frac{\partial^2 p}{\partial z^2} \right\} = 0 \tag{1.29}$$

1.1.6 Two-Dimensional wave equation in Cylindrical coordinates

To convert equation (1.29) from (x, z) to (r, θ) coordinates,

$$x = r\cos\theta, z = r \ \ and \ t = t \tag{1.30}$$

Every (x, z, t) will map to a unique (r, θ, t). The Jacobian of the transformation is

$$\mathbf{J} = \frac{\partial(x.z,t)}{\partial(r,\theta,t)} \tag{1.31}$$

$$= \begin{pmatrix} \frac{\partial x}{\partial r} & \frac{\partial x}{\partial \theta} & \frac{\partial x}{\partial t} \\ \frac{\partial z}{\partial r} & \frac{\partial z}{\partial \theta} & \frac{\partial z}{\partial t} \\ \frac{\partial t}{\partial r} & \frac{\partial t}{\partial \theta} & \frac{\partial t}{\partial t} \end{pmatrix} \tag{1.32}$$

$$= \begin{pmatrix} \cos\theta & -r\sin\theta & 0 \\ \sin\theta & r\cos\theta & 0 \\ 0 & 0 & 1 \end{pmatrix} \tag{1.33}$$

We have $J = |\mathbf{J}| = r$, so the transformation is singular and thus nonunique when $r = 0$. It is orientation-preserving for $r > 0$, and it is volume preserving only for $r = 1$; thus, in general it does not preserve volume. (Powers 2017).

The metric tensor **G** is

$$\mathbf{G}=\mathbf{J}^{T}.\mathbf{J}, \tag{1.34}$$

$$=\begin{pmatrix} \cos\theta & \sin\theta & 0 \\ -r\sin\theta & r\cos\theta & 0 \\ 0 & 0 & 1 \end{pmatrix}\begin{pmatrix} \cos\theta & -r\sin\theta & 0 \\ \sin\theta & r\cos\theta & 0 \\ 0 & 0 & 1 \end{pmatrix} \tag{1.35}$$

$$= \begin{pmatrix} 1 & 0 & 0 \\ 0 & r^{2} & 0 \\ 0 & 0 & 1 \end{pmatrix} \tag{1.36}$$

Because **G** is diagonal, the new coordinates axes are also orthogonal. Now it can be shown that the gradient operator in the Cartesian system is related to that of the cylindrical system via

$$\nabla = \begin{pmatrix} \frac{\partial}{\partial x} \\ \frac{\partial}{\partial z} \\ \frac{\partial}{\partial t} \end{pmatrix} = (\mathbf{J}^{T})^{-1} \begin{pmatrix} \frac{\partial}{\partial r} \\ \frac{\partial}{\partial \theta} \\ \frac{\partial}{\partial t} \end{pmatrix}, \tag{1.37}$$

$$= \begin{pmatrix} \cos\theta & -\frac{\sin\theta}{r} & 0 \\ \sin\theta & \frac{\cos\theta}{r} & 0 \\ 0 & 0 & 1 \end{pmatrix} \begin{pmatrix} \frac{\partial}{\partial r} \\ \frac{\partial}{\partial \theta} \\ \frac{\partial}{\partial t} \end{pmatrix}, \tag{1.38}$$

$$= \begin{pmatrix} \cos\theta\frac{\partial}{\partial r} - \frac{\sin\theta}{r}\frac{\partial}{\partial \theta} \\ \sin\theta\frac{\partial}{\partial r} + \frac{\cos\theta}{r}\frac{\partial}{\partial \theta} \\ \frac{\partial}{\partial t} \end{pmatrix} \tag{1.39}$$

Consider then the Lablacian operator, $\nabla^{2}= \nabla^{T}.\nabla$, which is

$$= \left(\cos\theta\frac{\partial}{\partial r} - \frac{\sin\theta}{r}\frac{\partial}{\partial\theta} \quad \sin\theta\frac{\partial}{\partial r} + \frac{\cos\theta}{r}\frac{\partial}{\partial\theta} \quad \frac{\partial}{\partial t}\right)\begin{pmatrix}\cos\theta\frac{\partial}{\partial r} - \frac{\sin\theta}{r}\frac{\partial}{\partial\theta}\\ \sin\theta\frac{\partial}{\partial r} + \frac{\cos\theta}{r}\frac{\partial}{\partial\theta}\\ \frac{\partial}{\partial t}\end{pmatrix} \tag{1.40}$$

Detailed expansion followed by extensive use of trigonometric identities reveals that equation (1.40) reduces to

$$\nabla^T.\nabla = \nabla^2 = \frac{1}{r}\frac{\partial}{\partial r}\left(r\frac{\partial}{\partial r}\right) + \frac{1}{r^2}\frac{\partial^2}{\partial\theta^2} + \frac{\partial^2}{\partial t^2} \tag{1.41}$$

1.1.7 Solutions of the wave equation in cylindrical coordinates

In this section the solutions of the wave equation in cylindrical coordinates as given in equation (1.41) will be formulated. A standard technique often utilised to solve PDE of this type is the separation of variables. (Arfken and Weber (2001)). The solution of a PDE can be written in terms of a product of functions which only dependent on one variable. Applying this principle to equation (1.41) states that the solution can be written as a product of functions which are only dependent from one of the three spatial variables θ, r, z and the time t as

$$p(\theta, r, z, t) = p_\theta(\theta), p_r(r).p_z(z), p_t(t) \tag{1.42}$$

Introducing the solution equation (1.42) into the wave equation (1.41), results in three ordinary differential equations of second order for $p_\theta(\theta), p_r(r).p_z(z)$, and $p_t(t)$. The solution to the radial part $p_r(r)$ is given by Bessel's differential equation (Williams (1999)).

$$\frac{d^2p(r)}{dr^2} + \frac{dp_r(r)}{rdr} + \left(k_r^2 - \frac{v^2}{r^2}\right)p_r(r) = 0 \tag{1.43}$$

The solutions of Bessel's differential equation are given by the Bessel functions of first, second and third kind.

$$p_r(r) = R_1 J_n(k_r r) + R_2 Y_n(k_r r) \quad (1.44)$$

where R_1, R_2 are arbitrary constants. The Bessel functions of the first kind and non-negative integer degree n of r denoted by $J_n(.)$ are solutions of Bessel's differential equation that are finite at the origin $r = 0$. They can be defined by its Taylor series expansion around $r = 0$ as follows (Williams 1999)

$$J_n r = \sum_{m=0}^{\infty} \frac{(-1)^m}{m!\Gamma(m+n+1)} \left(\frac{r}{2}\right)^{2m+n} \quad (1.45)$$

where $\Gamma(.)$ Is the gamma function, a generalisation of the factorial function to non-integer values. Bessel function behaviour looks like oscillating sine or cosine functions that decay proportionally to $1/\sqrt{x}$. for integer order, the following relationship is valid

$J_{-n}(x) = (-1)^n J_n(x)$ (williams1999)

1.1.8 Numerical Solution

For simulation of time dependent acoustic, electromagnetic or elastic wave phenomena, the efficient and accurate numerical solution of the wave equation is of fundamental importance. Finite difference methods are commonly used for simulation of time dependent waves because of their simplicity on structured Cartesian meshes. However, in the presence of complex geometry or small geometric features that require locally refined meshes their usefulness is somewhat limited. In contrast, finite element methods (FEMs) easily handle locally refined unstructured meshes and their extension to high order is straightforward even in the presence of curved boundaries

or materials interfaces, this is according to Wang *et al* (2010). When a second order hyperbolic problem is discretized by the use of Galerkin which is a finite element method, the problem typically leads to a second order system of ordinary differential equations.

The numerical solutions of wave propagation have numerous applications. One of particular interest is to simulate seismic surveys in oil and gas explorations. Various numerical methods have been developed to carry out this simulation. In this thesis an implementation of the discontinuous Galerkin finite element time domain method (DGTD) is applied to acoustic wave equation in cylindrical symmetry and MATLAB computer program to evaluate its accuracy and efficiency is used.

1.1.9 Seismology in oil Industry

In heterogeneous media, the speed and density of sound wave varies in one or more space coordinates. In cases where the variation occurs as discrete discontinuities in the medium properties, the derivation of the linear wave equation is not valid at discontinuity itself, and the problem therefore has to be formulated as a boundary value problem. For continuously varying media, the space dependency is directly included in the wave equation. This is according to Jensen et al (2011)

The ocean environment in reality is a combination of the two, with the medium properties changing abruptly at the scabbed and at sub bottom interfaces between different geological strata, but with speed of sound varying more or less continuously in the water column. However, since the analytical approach is different in the two cases, we will describe the solution of the wave equation in discretely and continuously varying media separately. The numerical approaches, in general, have to

combine the treatment of these two types of medium heterogeneity. (Jensen et al 2011)

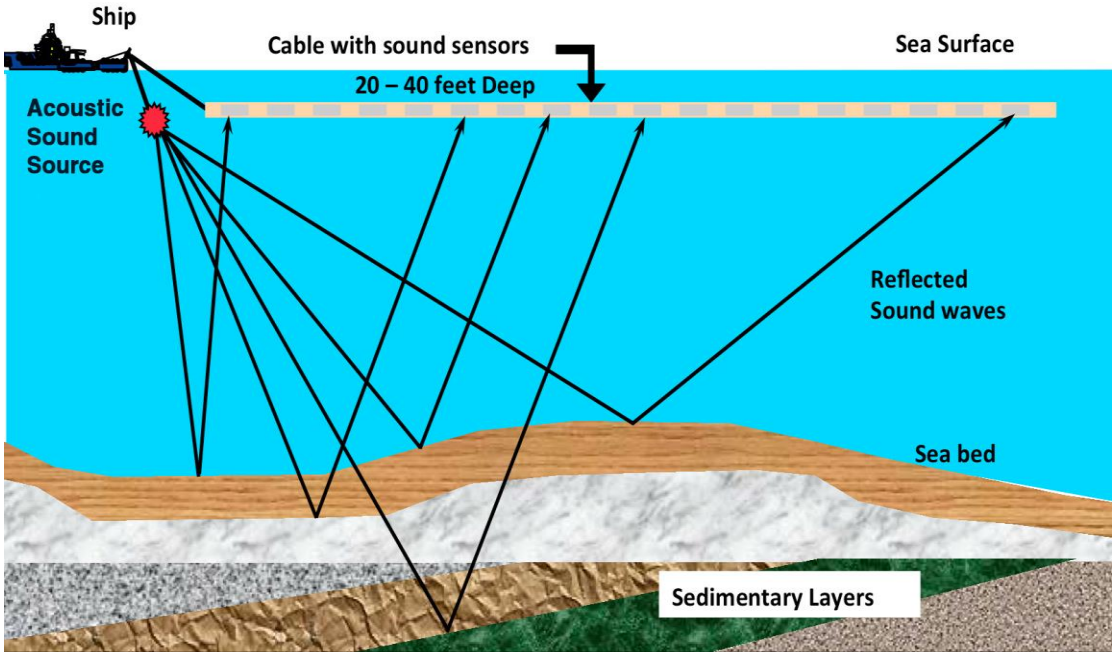

Figure 1.1 Seismic survey

The figure above illustrates the heterogeneity of the sea to the sea bed and the movement of the sound wave from ship guns as the acoustic sound source. The sound wave hit the sea bed and reflects back depending on the nature of the sea bed. The reflected sound wave, is received by a cable with sound sensors.

The reflected sound wave help scientists map the ocean floor and geology beneath it. Surveyors release compressed air into the water to create short duration sound waves that reflect off subsurface rock layers and are received by sensors being towed behind the vessel. The collected data is analyzed by scientists and used to create maps of geological structures that could contain energy resources beneath the ocean floor. The sound produced during seismic surveys is comparable in magnitude to many naturally occurring and other man-made ocean sound sources, including wind and wave action, rain, lightning strikes, marine life, and shipping. This is according to Symes (2003).

Survey operations are normally conducted at a speed of approximately 4.5 to 5 knots (~5.5 mph), with the sound source typically activated at 10-15 second intervals. As a result, the sound does not last long in any one location and is not at full volume 24 hours a day.

1.2 Statement of the Problem

To accurately handle wave propagation on the surface of a cylindrical domain, discontinuous Galerkin time domain method which is a Finite Element method is used in this research to solve the 2-D acoustic wave equation in cylindrical coordinates (r, θ, t), along the radial direction $r \in [1,2]$ over radial angle $\theta \in [0^o, 30^o]$.

1.3 General objective

The goal of this study is to solve the acoustic wave problem using the Discontinuous Galerkin time domain method of approximation by finding a function which satisfies the given PDE's and the boundary conditions and then compare with the exact solution obtained from Bessel function of the first kind.

1.4 Objectives of the Study

Objectives of the research include;

1. Solve the 2-D acoustic wave problem in cylindrical coordinates using Discontinuous Galerkin time domain approach of approximation which is a finite element method.
2. Using the free surface and absorbing boundary conditions, analyse the solution of pressure values for the acoustic wave equation along the radial direction over radial angle on the nodal points in the domain.

3. Compare the exact result based on the Bessel function of the first kind and the numerical result of the acoustic wave propagation in terms of accuracy.

1.5 Significance of the Study

Acoustics is the science of sound, including its production, transmission and effects. It is distinguished from optics in that sound is a mechanical, rather than an electromagnetic, wave motion. The broad scope of acoustics is an important area of interest and study to a variety of reasons. First, there is the ubiquitous nature of mechanical radiation, generated by natural causes and human activity and then second, there is the existence of the sensation of hearing, of the human vocal ability, of communication via sound, along with the variety of psychological influences sound has on those who hear it. This is according to a study done by Pierce (2019). It is also a significant factor especially in underwater acoustics. A variety of applications, in basic research and in technology, exploit the fact that transmission of sound is affected by, and consequently gives information concerning, the medium through which it passes and intervening bodies and in homogeneities. (Pierce 2019).

During oil and gas explorations either in land or sea, the first step is to conduct seismic surveys, which typically consist of sending into the ground sound waves generated by sources at the sea or ground surface such as air guns in marine surveys or dynamite in land acquisition and through sensors called geophones recording echoes of the sending waves, caused by the heterogeneity of the earth's subsurface. The recorded time series of data called seismic traces or seismograms is then analyzed by seismologists and geoscientists and interpret the earth's interior properties by imaging technologies based on the basic mathematical point of view that "waves transfer space-time resolved information from one place to another with (relatively) little loss. This is according to Symes (2003).

The resulting numerical solution can be applied in the evaluation of the effects of the cavities on seismograms recorded in boreholes or in cylindrical shaped tunnels in oil and gas exploration either in land or sea.

CHAPTER TWO

LITERATURE REVIEW

This is a presentation of brief discussions of various works done in the line of the present study, their breakthroughs, challenges and limitations.

2.1 Solution for acoustic wave equation

The solution to scalar wave equation using Standard Finite difference methods have been implemented as part of CREWES Matlab toolbox by Youzwishen and Margrave (1999) and Margrave (2000). These implementations handle a variety of simple boundary conditions.

A mathematical model of linear acoustic wave propagation in fluids has been presented by Mohamed *et al* (2011). The approach is based on an analytical solution to the homogenous wave equation for fluid medium. Normal mode analysis in a medium with 2-D spatially-variable acoustic properties for the propagation of acoustic pressure wave has been explained. This normal mode method analysis gives exact solutions without assumed restrictions on pressure and velocity.

According to Atangana (2013), the solution of an acoustic wave equation with Variable-Order derivative loss operator has been presented. The use of fractional derivatives when modelling sound propagation, leads to models that better describe observations of attenuation and dispersion. The wave equation for viscous losses involving interger-order derivatives only leads to an attenuation which is proportional to the square of the frequency. The Crank-Nicholson scheme solves the generalised equation.

In the journal; Operator upscaling for acoustic wave equation by Tetyana *et al* (2005), upscaling is the process of redefining the physical system's parameters up to a coarser

grid, forming effective or equivalent parameters. Modelling of wave propagation in a heterogeneous medium requires input data that varies on many different spatial and temporal scales. Operator based upscaling captures the effect of the fine scales on a coarser domain without solving the full fine-scale problem. The method applied to the constant density, variable sound velocity acoustic wave equation, consists of solving small independent problems for approximate fine-scale information internal to each coarse block and using these sub-grid solutions to define an upscaled operator on the coarse grid.

2.2 Galerkin Method

Galerkin method was invented by a Russian Mathematician, Boris Grigoryerich Galerkin. Galerkin methods are a class of methods for converting continuous operator problem (such as a differential equation) to a discrete problem. In principle, it is equivalent of applying the method of variation of parameters to a function space with a finite set of basis functions. Galerkin methods developed in engineering have now been used in many diverse applications including meteorology, oceanology and many other scientific disciplines that require tracking various wave phenomena.

Considerable research has been undertaken in recent times to solve hyperbolic problems to develop optimal methods with respect to local polynomial degree p. The resulting methods have hence been termed hp-finite element methods.

The comparison between continuous piecewise polynomials and their discontinuous versions can be found in Houston *et al* (2002), where a least squares stabilization method is proposed for discontinuous Galerkin methods.

In the Galerkin approach, the problem is reformulated by requiring the equation residual to be orthogonal to each of the basic functions that are chosen. The basis functions satisfy the natural boundary conditions.

2.3 Discontinuous Galerkin time domain approach

Reed and Hill (1973) proposed the first Discontinuous Garlekin finite element method as an approach for solving the neutron transport equation and as a solution to overcome the stability limitations of conventional continuous finite element approximations to first order hyperbolic problem. After its introduction, the DG laid dormant for many years. However, in the past two decades, there has been renewed interest in the class of methods stimulated by computational convenience of DG due to the need to approximate advection-dominated diffusion problems without excessive numerical stabilization and the desire to handle nonlinear hyperbolic problems which are known to exhibit discontinuous solution even when the data is smooth.

On the other hand, Erickson and Johnson (1991), published a series of papers analysing the DG method applied to parabolic problems where they focused on the heat equation by adopting the DG method in time and the standard Galerkin method space.

Cockburn and Shu (1998), extended the DG method to solve first-order hyperbolic partial differential equations of conservation laws. The authors developed later the local discontinuous Galerkin method for convention-diffusion problems.

Atkins and Shu (1998) and Hesthaven and Warburton (2007) propose efficient quadrature-free DG implementation strategies in the case of piecewise constant media on triangular meshes. Aside from reduction in code complexity and overhead computational cost, these quadrature-free implementations result in lower memory

costs associated with storing DG operators relative to their quadrature based counterparts. On the other hand, quadrature based implementations have the upper hand in terms of accuracy since medium parameters as variable functions in space within mesh elements are better representatives than piecewise constant coefficients when computing element wise integrals in the definition of DG operators such as mass and stiffness matrices. For example, Ober *et al.* (2010) employ quadrature based DG implementations in the context of acoustic seismic inversion. A comparison between the quadrature-free and quadrature based DG implementations for elastic wave propagation in variable media is provided. Their results show that the numerical solutions for piecewise constant and variable models do not converge to the same limit as the polynomial order is increased. However, insight into the performance and efficiency of quadrature-free and quadrature based implementations is not provided. Arnord *et al* (2001), provide a framework for analysis of wide class of discontinuous methods for second order elliptic problems. This analysis permits scientists to have a detailed recapitulation and comparison of discontinuous Galerkin methods proposed over the last few decades for the numerical treatment of elliptic problems.

The DG method has been evaluated in several studies including the modelling of shallow water equations (Eskilsson and Shervin 2005), compressible and incompressible Navier-stokes equations (Shahbazi *et al* 2007). The active development of the DG method in the last few years proves their efficiency in a wide range of applications. They have been used to solve complex problems in areas of compressible and incompressible flows, transport equations and viscoelastic fluid flow, turbo machinery flows, magneto-hydrodynamics including Maxwell`s equation, semi-conductor device simulation, transport of contaminant in porous media, second order elliptic problem and elasticity.

Grote *et al* (2006), presented the symmetric interior penalty discontinuous Galerkin (SIPDG) method for the numerical discretization of second order scalar wave equation. They used the SIPDG finite element method in space while leaving the time dependence continuous.

Celiker and Cockburn (2007) studied the discontinuous Galerkin, Petro-Galerkin and hybridized mixed methods for convection-diffusion problems in one space.

Kaser and Dumbser (2006) presents a new numerical approach to solve the elastic wave equation in heterogeneous media in the presence of externally given source terms with arbitrary high-order accuracy in space and time on unstructured triangular meshes. A discontinuous Galerkin method is combined with the ideas of the ADER time integration approach using arbitrary high-order derivatives. The time integration is performed via the so-called Cauchy-kovalewski procedure using repeatedly governing partial differential equation itself.

Klockner *et al* (2009) extended the DG method to run on graphics processing units to approximate the time-dependent Maxwell's equation in realistic 3D problems. The results predict that computation time is largely decreased when the DG method is computed on graphics processing unit.

Wang *et al* (2010), compared DG and FD methods for time domain acoustics, results reveal the efficiency of the DG method over staggered FD methods for the case of complex piecewise constant media. Interface errors over the discontinuity reduce the convergence rate of FD methods to first order, while a DG scheme with an appropriately aligned mesh results in a sub-optimal second order method making DG a more efficient method for complicated models.

Another interesting study was conducted by Simonaho *et al* (2012), where DG simulation of acoustic wave propagation were compared to real data. The author simulated an acquired 3D experimental data for pulse propagation and scattering from a cylinder in air. Results show that simulated data matches measurement time-series well up to 4.5 m/s for the pulse propagation study. Moreover, amplitude spectrum of the simulated data closely resembles that of real data for frequencies less than 2 kHz. For the scattering cylinder case, simulated data contained all of the representative qualitative characteristics present in the real data, which is interference patterns from reflections and diffractions due to the cylinder, for 2D spatial slices at given time-shots. A lot of the work on DG applied to wave propagation cited above, assumes that the medium parameters are piecewise constant for implementation purposes.

Zhebel *et al* (2013) perform a study on the parallel scalability of FD and finite element method, including mass lumped finite elements and DG, for 3D acoustic wave propagation in piecewise constant media with a dipping interface on an Intel Sandy Bridge dual 8-core machine and Intel's 61-core Xeon Phi. Overall the DG method demonstrated larger speed up on Sandy Bridge as the number of cores was increased and the problem size is kept constant, partly due to the fact that DG involves more net FLOPs (floating point operations) relative to other methods. Interestingly enough, for Intel's Xeon Phi, FD and DG methods showed similar strong scalability performance, for an optimal choice of FD domain subdivisions. Lastly, convergence results by Zhebel *et al* (2013) demonstrate again the superior accuracy of finite element type methods with mesh alignment to that of FD methods.

The propagation of small perturbations in complex geometries can involve hydrodynamic-acoustic interactions, coupling acoustic waves and vertical modes. Renzo (2016), proposed a propagation model, based on the linearized Navier-stokes

equations. It includes the mechanism responsible for generation of vorticity associated with the hydrodynamic modes. The linearized Navier-stokes equations are discretised in space using a discontinuous Galerkin formulation for unstructured grids.

Wang (2017) performed a study on Finite Difference and Discontinous Galerkin methods for wave equations. Wave propagation problems can be modelled by partial differential equations. Wave propagation in fluids and in solids is modelled by the acoustic wave equation and the elastic wave equation respectively. In real world applications, wave often propagates in heterogeneous media with complex geometries, which makes it impossible to derive exact solutions to the governing equations. An efficient numerical method produces accurate approximation at low computational cost. The finite difference method is conceptually simple and easy, but has difficulties in handling complex geometries of the computational domain according to the author. However, discontinuous galerkin method is flexible with complex geometries, making it suitable for multiphysics problems. An energy based discontinuous Galerkin method is used to solve a coupled acoustic-elastic problem.

From the review of the literature on previous studies, no study has been done to solve a 2-D wave equation particularly on cylindrical coordinates using discontinuous Galerkin time domain method which belongs to Finite Element method yet the method can be adopted to solve problems of complex geometry unlike other numerical methods. Hence this study is meant to fill the gap.

CHAPTER THREE

METHODOLOGY

In this chapter, various aspects of the research methodology are presented. A review on the numerical methods which include, Finite difference method, Finite volume method, Boundary element method and Finite element method. Galerkin method is a form of Finite element method, is used to find the approximate form of the governing equation expressed in cylindrical coordinates with appropriate initial and boundary conditions. The discretization of the appropriate grid is also given in this chapter.

3.1 Review on numerical methods

To find closed-form analytical solutions to canonical PDEs, the number of methods available is limited. The available methods include separation of variables, superposition, product solution methods, Fourier transforms, Laplace transforms and perturbation methods, which are limited by constraints such as regular geometry, linearity of the equation and constant coefficients. When these constraints are imposed of they severely curtail the range of applicability of analytical techniques for solving PDES, rendering them almost irrelevant for problems of practical interest. This is according to Sandip (2016). In realisation of this fact, numerous numerical methods have been proposed to solve different types of partial differential equations (PDEs) that describe the physical dynamics of the world. Three notable methods are Finite Difference Methods (FDMs), Finite Volume Methods (FVMs), Boundary element method (BEMs) and Finite Element Methods (FEMs). Two common FEMs are Continuous Galerkin (CG) and Discontinuous Galerkin (DG), each of which comprises an element-based approach to solving a set of equations. The main focus of this thesis is to explore DG method for approximating a 2-D wave equation with unique boundary conditions.

3.1.1. Finite Difference Method

The Finite difference method is based on the calculus of finite differences. According to Sandip (2016), in Finite difference method, the governing PDE is satisfied at a set of prescribed interconnected points within the computational domain, basically known as nodes, making the method relatively straightforward. The boundary conditions in turn are satisfied at a set of prescribed nodes located on the boundaries of the computational domain. The framework of interconnected nodes is referred to as grids or mesh. Each derivative in the PDE is approximated using a difference approximation that is typically derived using Taylor series expansions.

With the FD method, the discretization of general initial-boundary value problem is intuitively simple, which makes the approach very popular. The huge disadvantage of the FD method, however, is that the approach is highly ill-suited to deal with complex geometries of the computational domain. Despite the disadvantages of the FD method, it is still heavily investigated, especially in the field of therapeutic ultrasound and propagation of electromagnetic waves. Timo (2010))

3.1.2. Finite Volume Method

The finite volume method derives its name from the fact that in this method the governing PDE is satisfied over finite-sized control volumes, rather than at points. In this method, the first step is to split the computational domain into a set of control volumes known as cells. In general, these cells may be of arbitrary shape and size, although, traditionally, the cells are convex polygons (in 2D) or polyhedrons (in 3D), that is, they are bounded by straight edges (in 2D) or planar surfaces (in 3D). As a result, if the bounding surface is curved, it is approximated by straight edges or planar faces. These bounding discrete surfaces are known as cell faces or simply, faces. The

vertices of the cells, on the other hand, are called nodes, and are, in fact, the same nodes that were used in the finite difference method. All information is stored at the geometric centroids of the cells, referred to as cell centres. The derivation of the finite volume equations commences by integrating the governing PDE over the cells constituting the computational domain. (Sandip 2016)

3.1.3. Boundary Element Method

BEM is a method by which the external surface of the domain is divided or discretised into series of elements over which the function under consideration can vary in different ways, in much the same way as finite elements. According to Sandip (2016), the boundary element method (BEM) is a derivative of the finite element method. Its attractive feature is that it does not require a volumetric mesh, but only a surface mesh. This is particularly convenient for 2D geometries, wherein the only geometric input required is a set of coordinates of points. This method is particularly suited to problems for which the interior solution is not of practical interest. For PDEs with constant coefficients or in which the variation of the coefficients obey a certain format, boundary element method is only used. This is because it is only applicable to problems for which Green's functions can be computed easily. Nonlinear PDEs, PDEs with strong in homogeneities, and 3D problems are generally outside the realm of pure BEM. For BEM to be applied in such scenarios, usually it requires a volumetric mesh and combination of BEM with a volume discretization method, which undermines its advantage of being an efficient method. Due to these limitations BEM has found limited use except for some specific problems in mechanics, heat conduction and electrostatics. This is according to Sandip (2016).

3.1.4. The Finite Element Method

Finite element method is a numerical technique that gives approximate solutions to differential equations that model problems arising in physics and engineering. As with the more commonly used finite difference schemes, the finite element method reduces problems defined in geometrical space (or domain), to finding a solution in a finite number of points by subdividing the domain into smaller regions (a mesh). In finite elements, each sub region or "element" is unique and need not be orthogonal to the others. For example, triangles or quadrilaterals can be used in two dimensions, and tetrahedral or hexahedral in three dimensions. Over each finite element, the unknown variables like temperature, velocity and others are approximated using known functions; these functions are usually polynomials that can be linear or higher-order expansions based on the geometrical locations of a few points (nodes) used to define the finite element shape. In contrast to finite difference procedures (conventional finite differences, as opposed to the finite volume method, which is integrated), the governing equations in the finite element method are integrated over each finite element, and the contributions summed ("assembled") over the entire problem domain. As a consequence of this procedure, a set of finite linear equations is obtained in terms of the values of the unknown parameters at the elements nodes. Solutions of these equations are achieved using linear algebra techniques. (Darrell and Juan 2017)

Finite element method has essentially become the de facto standard for numerical approximation of the partial differential equations that define structural engineering, and presently it is widely accepted for a multitude of other engineering and scientific problems. Most of the commercial computer codes today are finite element based—even the finite volume computational fluid dynamics codes sold commercially employ

mesh generators based on finite element unstructured mesh generation. This is according to the study by Darrell and Juan (2017).

In this thesis the FE method was used to approximate the time-dependent acoustic wave equation in 2D problems. The underlying principle of the finite element method resides in the method of weighted residuals. The two most commonly used procedures are the Rayleigh–Ritz and Galerkin methods. Rayleigh–Ritz method is based on calculus of variations; however, the method cannot be used on some more complicated equations. The Galerkin method is simple to use and is guaranteed to yield a compatible approximation to the governing differential equation even when the Rayleigh–Ritz method cannot be applied. In both of the methods, the dependent variable is expressed by means of a finite series approximation in which the "shape" of the solution is assumed known, and it depends on a finite number of parameters to be determined. Replaced in the governing differential equation, the Galerkin approximation generates a residual function, which is multiplied by weighting functions and is required to be orthogonal to the weighting functions in the integrated sense. (Darrell and Juan 2017)

3.1.4.1 Galerkin Method

Galerkin Methods belong to a class of solution methods for PDE's where the solution residue is minimised giving rise to well-known weak formulation of problems. In this approach, according to Kythe *et al* (2003) a basis function of the form

$$u(x,t) = \phi_0(x) + \sum_{j=1}^{N} c_j(t)\phi_j(x) \quad (3.1)$$

is chosen where,

$\phi_j(x)$ is the finite number of basis functions.

c_j is unknown coefficients.

For a given differential equation of the form $L[u] = f,$ defined on a region Ω where L is a linear spatial differential operator and f is a given function, subject to boundary conditions $u = g(s)$ on Γ_1, and

$$\frac{\partial u}{\partial t} + k(s)u = h(s) \text{ on } \Gamma_2 \tag{3.2}$$

Where $\Gamma = \Gamma_1 \cup \Gamma_2$ is the boundary of the region Ω. A space of functions V is choosen in which element u and v will reside. The function u is written as a linear combination of the basis functions of the space,

$$u = \sum_i a_i \phi_i \, , \tag{3.3}$$

and v is choosen from amongst the basis functions. The measure of the residual (error) associated with an approximate solution is defined as $R[u] = L[u] - f$ should then theoretically be zero. That is,

$$\int_\Omega R[u] v \, dx = 0, \quad \text{for all } v \in C_0^1(\Omega)$$

or,

$$\sum_i a_i \int_\Omega L[\phi_i]\phi_j dx = \int_\Omega f \phi_j \, dx, \qquad \text{for all } j. \tag{3.4}$$

The Galerkin Method requires that the residual be orthogonal with respect to the basis functions ϕ_i i.e.

$$\langle R[u], \phi_i \rangle = 0 \tag{3.5}$$

The infinite sums according to Matt et al (2012), must be truncated at some large N, the intergrals evaluated and re-written as a large N-dimensional system of equations to be solved for the unknowns $a_i's$,

$$\boldsymbol{K}\mathrm{a}=\mathbf{f}\,. \tag{3.6}$$

According to Prem *et al* (2003), the formulation can be generalised to a 2-D case which becomes;

$$\iint_\Omega \{L[u]-f\}\phi_i\,dxdy=0 \qquad i=1,\ldots\ldots\ldots,N \tag{3.7}$$

or

$$\sum_{j=1}^{N} a_i \iint_\Omega \phi_i\, L\phi_j dxdy = \iint_\Omega f\phi_i dxdy \tag{3.8}$$

which in the matrix form is written as

$$[A]\{c\}=\{b\},$$

Where, $A_{ij}=\iint_\Omega \phi_i L\phi_j dxdy$, $b_i=\iint_\Omega f\phi_i\,dxdy$ also $[c]=\begin{Bmatrix}c_i\\c_j\end{Bmatrix}$

According to Benjamin (2015), the two main categories of Galerkin methods are Continuous Galerkin (CG) and Discontinuous Galerkin (DG). Both methods use an elemental approach to solving integral form, but the difference between DG and CG is mainly whether the continuity between the elements is enforced in a more general form i.e weak variational formulation or in the corresponding strong formulation.

A computational domain is build when using CG and then subdivided into various-sized elements, similar to FVM. Within each element however, we use specially selected degrees of freedom. For example, in the one-dimensional sense, the degrees of freedom could be a grid of points across the cell.(Benjamin 2015)

Generally, DG is similar to CG in requiring numerical interpolation and integration as well as building the same computational domain; one of the main differences however

comes from the elemental boundaries. The boundaries are required to be continuous in CG, while in DG they are discontinuous and the continuity is enforced weakly. According to Benjamin (2015), the domain in DG is still represented by a collection of elements; the union of these elements is accomplished through a numerical flux similar to FVMs. Similar to FEMs, Discontinuous Galerkin still uses the same space of basis and test functions, and each element boundary has its own set of degrees of freedom.

The solution therefore is typically represented by a set of piecewise polynomials that are discontinuous at the element boundaries. The numerical flux, resolves this discontinuity to assist in finding the final solution. Furthermore, the mass matrix is constructed locally instead of globally and this allows it to be inverted at a reduced computational cost, yielding a semi discrete scheme that is explicit. Discontinuous Galerkin is the method used in this research. (Benjamin 2015)

3.2 Discontinuous Galerkin Method for Acoustic wave equation

The discontinuous Galerkin (DG) method was originally introduced by Reed and Hill (1973). The idea of the DG method is to decompose the original problem into a set of sub problems that are connected using an appropriate transmission condition (known as the numerical flux). For geometric partitioning of the computational domain, the DG method uses standard disjoint finite element meshes. In the DG method, each element of the computational mesh determines a single sub problem.

By setting the material properties for each sub problem to be constant, the solution is calculated separately for each element of the computational mesh. The solution for the whole computational domain is achieved by summing over all the elements of the mesh.

3.2.1. The governing equation

From equation (1.41), the acoustic wave equation in 2-D cylindrical coordinates is given by,

$$\frac{1}{r}\frac{\partial}{\partial r}\left(r\frac{\partial p}{\partial r}\right)+\frac{1}{r^2}\frac{\partial^2 p}{\partial \theta^2}=\frac{1}{c^2}\frac{\partial^2 p}{\partial t^2} \quad \text{in } \Omega \tag{3.9}$$

where Ω is the domain, r is the radius, θ is the radial angle, p is the pressure field, c is the velocity of the acoustic wave in the acoustic media and t denotes time. (David and Dan 1990). . The two dimensional domain Ω is bounded by the boundary $\partial\Omega$. The acoustic wave equation models sound propagation in the sea in the presence of cylindrical symmetry.

For the numerical algorithm, we recast (3.9) as a system of three coupled first order equations given by

$$\frac{\partial}{\partial t}\begin{pmatrix} p \\ r\frac{\partial p}{\partial r} \\ \frac{\partial p}{\partial \theta} \end{pmatrix} = A\begin{pmatrix} p \\ r\frac{\partial p}{\partial r} \\ \frac{\partial p}{\partial r} \end{pmatrix} + B\begin{pmatrix} p \\ r\frac{\partial p}{\partial r} \\ \frac{\partial p}{\partial r} \end{pmatrix} \tag{3.10}$$

Where $A=\begin{pmatrix} 0 & \frac{c^2}{r} & 0 \\ r & 0 & 0 \\ 0 & 0 & 0 \end{pmatrix}$ and $B=\begin{pmatrix} 0 & 0 & \frac{c^2}{r^2} \\ 0 & 0 & 0 \\ 1 & 0 & 0 \end{pmatrix}$

The numerical algorithm solves equation (3.9) with the free surface boundary condition at $r=a$ and with the absorbing boundary condition at the edges of the grid at $r=b$. The variables are discretised on a spatial grid which is non-uniform in the r direction and uniform in the θ variable.

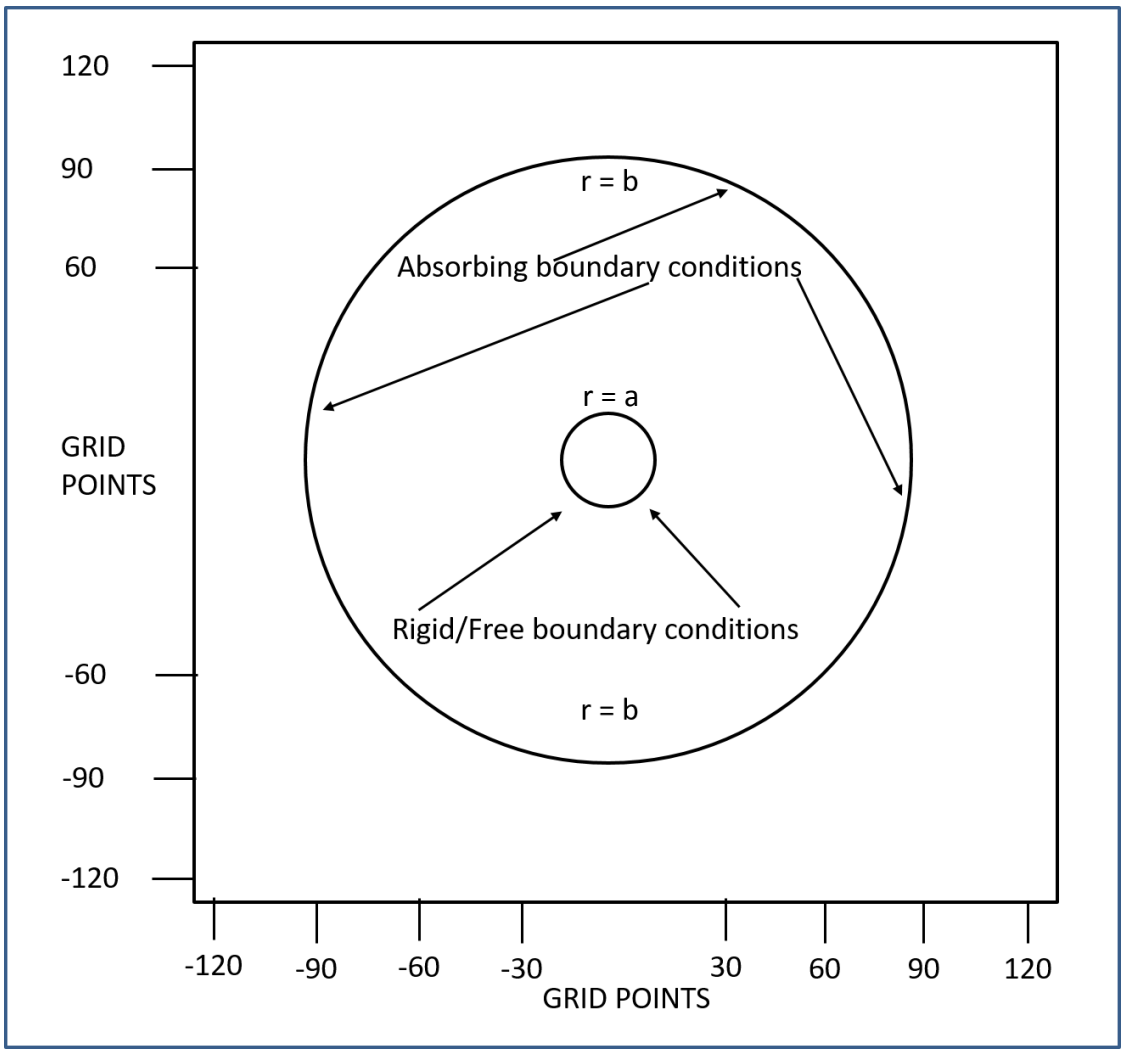

Figure 3.1 Configuration of boundary conditions

A cylindrical bar of radius $r = b$ is sliced through to show geometry of six equally-spaced symmetrical planes of angle $\theta = 30^o$. A unit cell will be discretised to triangular elements by subdividing the domain into triangular shaped units.

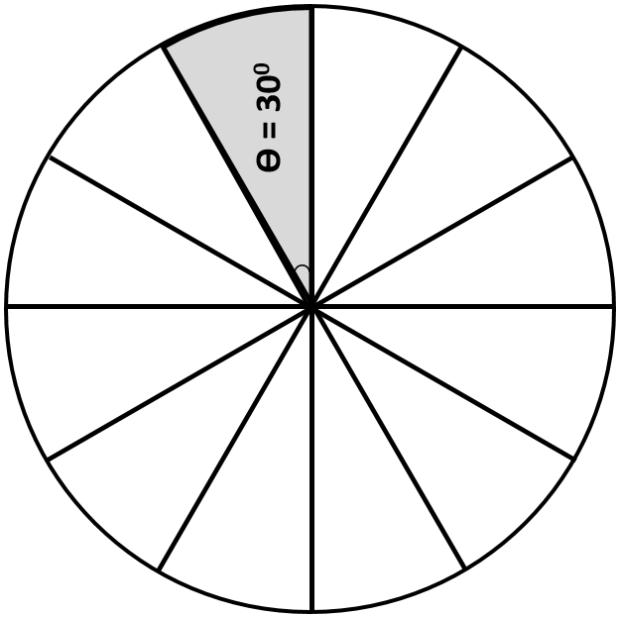

Figure 3.2 Slice through Cylindrical bar showing geometry, six equally-spaced planes of symmetry and unit cell (shaded)

3.2.2. Initial Condition

The initial condition $r = 0$ models the acoustic source at $t = 0$ and at $\theta = 0^o$

The expression $p(r, \theta, t)$ denotes the wave disturbance at angle θ over radius r.

The exact solution for this problem, using Bessel function of the first kind is;

$$p(r, \theta, t) = 100\, J_0(r) \sin(\frac{\pi t}{4}) \sin 3\theta \tag{3.11}$$

Hence at $t = 0$. the initial condition for pressure becomes $p(r, \theta, 0) = 0$

3.2.3. Boundary Conditions

There are two types of boundary conditions exclusively used in the seismic simulation, the free surface boundary condition and the absorbing boundary condition. The numerical simulation is carried out on a bounded domain whose boundaries are either the physical sea surface, landform or the fields far away from the domain of interest.

The absorbing boundary condition does not mimic any physical scenarios, but is used to truncate the open domain problem into a finite one so that the numerical method can handle. To solve equation (3.9) the free surface boundary condition at $r = a$ (see figure 3.1) and the absorbing boundary condition at the edges of the grid at $r = b$ are used. The variables are discretised on a spatial grid which is non-uniform in the r direction and uniform in the θ variable.

With changing radius at $\theta = 0$, using Bessel function of the first kind (equation (3.11)), we obtain pressure values at the right hand boundary of the domain at $t = 1$ as given below;

$$p(1,0,1) = 0\,; \qquad r = 1$$

$$p(1.5,0,1) = 0\,; \qquad r = 1.5$$

$$p(2,0,1) = 0\,; \qquad r = 2$$

With changing radius at $= \frac{\pi}{6}$, using Bessel function of the first kind (equation (3.11)), we obtain pressure values at the left hand boundary of the domain at $t = 1$ as given below;

$$p\left(1,\frac{\pi}{6},1\right) = 54.11; \qquad r = 1$$

$$p\left(1.5,\frac{\pi}{6},1\right) = 36.19\,; \qquad r = 1.5$$

$$p\left(2,\frac{\pi}{6},1\right) = 15.83\,; \qquad r = 2$$

3.2.4. The appropriate grid

The figure below shows finite mesh showing discretization of the unit cell for the cylindrical bar using triangular elements

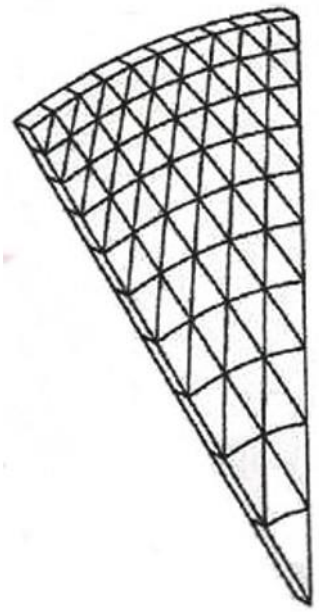

Figure 3.3 Finite element mesh showing discretization of the unit cell.

The unit bar above is $r = 2$ and $\theta = \frac{\pi}{6}$. The free surface boundary is at $r = 1$ and the absorbing boundary is at the edges of the grid at $r = 2$. The domain is discretised into 8 triangular elements as shown in the figure below

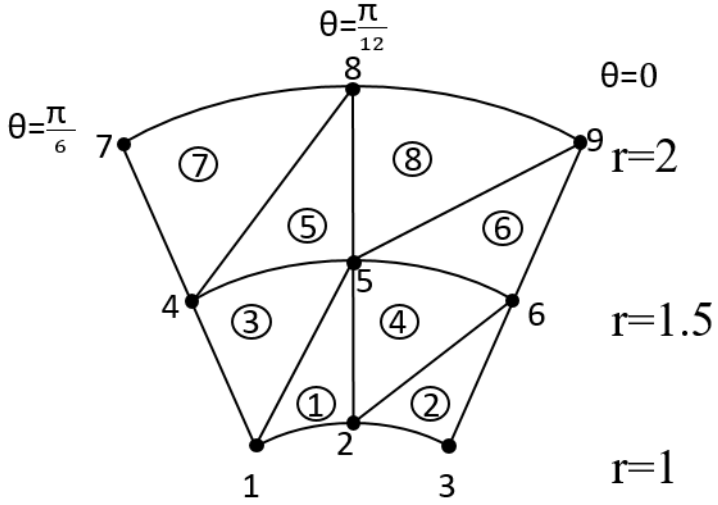

Figure 3.4– Triangulation of a surface Domain

3.2.5. Formulation of DG method for 2D acoustic wave equation

The exact solution to equation (3.9) in cylindrical coordinates using Bessel function J_0 is given as equation (3.11), $u = (r, \theta, t)$ is the numerical approximation to $p(r, \theta, t)$. According to Jain (1986), to formulate and solve equation (3.9) using Discontinuous Galerkin approach, first we find the functional that corresponds to the partial differential equation (3.9) in (x, z, t), then the result is converted to suit the cylindrical coordinates (r, θ, t).

$$J[p] = \frac{1}{2}\iint_{\Omega}\left[\left(c^2\left(\frac{\partial^2 p}{\partial x^2}+\frac{\partial^2 p}{\partial z^2}\right)\right)-\frac{\partial^2 p}{\partial t^2}\right]dxdz = minimum$$

$$= \frac{1}{2}\iint_{\Omega}\left[c^2\left(\left(\frac{\partial p}{\partial x}\right)^2+\left(\frac{\partial p}{\partial z}\right)^2\right)-\left(\frac{\partial p}{\partial t}\right)^2\right]dxdz = 0 \qquad (3.12)$$

Where the boundary conditions are to be satisfied. We divide the domain Ω into finite elements as shown in the figure 3.3. The approximate solution $u(x,z,t)$ for the whole domain Ω in Cartesian coordinates may be written as

$$u(x,z,t) = \sum_{e=1}^{m} N^{(e)}\phi^{(e)} = \sum_{i=1}^{m} N_i\phi_i = N\phi \qquad (3.13)$$

where m is the number of elements with N nodes in $\Omega, N = [N_1, N_2 \dots \dots \dots N_m]$, $\phi = [\phi_1, \phi_2, \dots \dots \dots \phi_m]^T$ the basis functions N_i satisfy the conditions

$$N_i(x,z) = \begin{cases} N_i^{(e)}(x,z), & if\ (x,z) \in (e)\ and\ has\ i\ as\ an\ apex \\ 0, & otherwise \end{cases} \qquad (3.14)$$

and $\phi^{(e)}$ are the nodal values associated with the element (e).

The Galerkin method for the differential equation (3.12) may be written as

$$\iint_{\Omega(e)} N_i \left[c^2 \left(\frac{\partial}{\partial x}\left(\frac{\partial p^{(e)}}{\partial x}\right) + \frac{\partial}{\partial z}\left(\frac{\partial p^{(e)}}{\partial z}\right)\right) - \frac{\partial}{\partial t}\left(\frac{\partial p^{(e)}}{\partial t}\right)\right] dxdz = 0 \qquad (3.15)$$

$$i = 1,2 \dots \dots \dots q$$

Where N_i are the shape functions defined piecewise element by element and q is the number of unknown nodal quantities assigned to the element (e).

Before substituting for $p^{(e)}$ we express the first and second terms in the integrand in the form

$$\iint_{\Omega(e)} N_i \left[c^2 \left(\frac{\partial}{\partial x}\left(\frac{\partial p^{(e)}}{\partial x}\right)\right)\right] dxdz =$$

$$\int_{\partial\Omega(e)} N_i c^2 \frac{\partial p^{(e)}}{\partial x} n_x d_s + \iint_{\Omega(e)} c^2 \frac{\partial N_i}{\partial x}\frac{\partial p^{(e)}}{\partial x} dxdz$$

$$\iint_{\Omega^{(e)}} N_i \left[c^2 \left(\frac{\partial}{\partial z} \left(\frac{\partial p^{(e)}}{\partial z} \right) \right) \right] dxdz$$

$$= \int_{\partial\Omega^{(e)}} N_i c^2 \frac{\partial p^{(e)}}{\partial z} n_z d_s + \iint_{\Omega^{(e)}} c^2 \frac{\partial N_i}{\partial z} \frac{\partial p^{(e)}}{\partial z} dxdz$$

where $\partial\Omega^{(e)}$ is the boundary of the element (e), s is the coordinate on the boundary, n_x and n_z are the x and z components of outward normal of the boundary.Replacing the above expressions in equation (3.15) we get

$$\iint_{\Omega^{(e)}} \left[c^2 \left(\frac{\partial N_i}{\partial x} \frac{\partial u^{(e)}}{\partial x} + \frac{\partial N_i}{\partial z} \frac{\partial u^{(e)}}{\partial z} \right) \right] dxdz + \int_{\partial\Omega^{(e)}} N_i c^2 \frac{\partial u^{(e)}}{\partial n} ds = 0 \qquad (3.16)$$

where n is the unit outward normal.

This method can be regarded as analysing conditions at a particular instant of time, which is treating the derivatives with respect to the time variable as a constant in the formulation, since there is no integration with respect to time in equation (3.15). Jain (1986))

The time derivative $\frac{\partial p}{\partial t}$ is treated as a constant, the resulting differential equation contain time derivatives of the nodal values of p. Thus we obtain a system of linear ordinary differential equations in the p_i. The value of p within the element (e) is as shown in the figure below.

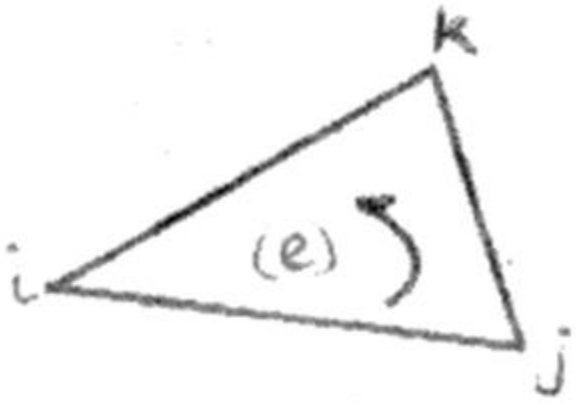

Figure 3.5; Triangular element

which is given by; $p^{(e)} = N_i p_i + N_j p_j + N_k p_k$

$$= \begin{bmatrix} N_i N_j N_k \end{bmatrix} \begin{bmatrix} p_i \\ p_j \\ p_k \end{bmatrix} = N^{(e)} \phi^{(e)} \tag{3.17}$$

So we can use

$$\frac{\partial p^{(e)}}{\partial t} = N_i \frac{dp_i}{dt} + N_j \frac{dp_j}{dt} + N_k \frac{dp_k}{dt} \tag{3.18}$$

in the approximate minimisation of equation (3.15) treating $\frac{\partial u^{(e)}}{\partial t}$ as a constant and using (3.17) and (3.18), we now substitute (3.12) into (3.16) and write the element equation as

$$\iint_{\Omega^{(e)}} \left[c^2 \left(\frac{\partial N^{(e)T}}{\partial x} \frac{\partial N^{(e)}}{\partial x} + \frac{\partial N^{(e)T}}{\partial z} \frac{\partial N^{(e)}}{\partial z} \right) \phi^{(e)} \right] dxdz + \int_{\partial\Omega^{(e)}} \left[N^{(e)T} c^2 \frac{\partial N^{(e)T}}{\partial n} \phi^{(e)} \right] ds -$$

$$\iint_{\Omega^{(e)}} \left[N^{(e)T} N^{(e)} \frac{d\phi^{(e)}}{dt} \right] dxdz = 0 \tag{3.19}$$

which may be written as;

$$A^{(e)} \phi^{(e)} + \int_{\partial\Omega^{(e)}} \left[N^{(e)T} c^2 \frac{\partial N^{(e)}}{\partial n} \phi^{(e)} \right] ds - b^{(e)} \phi^{(e)} = 0 \tag{3.20}$$

The term $\int_{\partial\Omega^{(e)}}\left[N^{(e)T}c^2\frac{\partial N^{(e)}}{\partial n}\phi^{(e)}\right]ds$ contributes to the vector $b^{(e)}$ when the derivative boundary conditions are associated with the differential equation (3.9) otherwise it is neglected.

Thus the element equation becomes;

$$A^{(e)}\phi^{(e)} - b^{(e)}\phi^{(e)} = 0 \tag{3.21}$$

Where; $\left\{A^{(e)} = \iint_{\Omega^{(e)}}\left[c^2\left(\frac{\partial N^{(e)T}}{\partial x}\frac{\partial N^{(e0}}{\partial x} + \frac{\partial N^{(e)T}}{\partial z}\frac{\partial N^{(e)}}{\partial z}\right)\right]dxdz,\ \ b^{(e)} = \iint_{\Omega^{(e)}}\left[N^{(e)T}N^{(e)}\frac{d\phi^{(e)}}{dt}\right]dxdz\ \ and\ \phi^{(e)} = \left[p_i, p_j, p_k\right]^T\right\}$ (3.22)

We then consider a three node triangular element (e) with nodes i, j, k as shown in Figure 3.5

Although many kinds of elements can be used, our treatment will consider triangular elements. The elements must span the entire region and approximate the boundary relatively closely. Every node (the vertices of our triangular elements) and every side of the triangles must be common with adjacent elements, except for sides on the boundaries.

The linear piecewise approximate solution over the element (e) may be written as

$$p^{(e)} = N_i p_i + N_j p_j + N_k p_k = N^{(e)}\phi^{(e)} \tag{3.23}$$

Where $N^{(e)} = \left[N_i, N_j, N_k\right],\qquad \phi^{(e)} = \left[p_i, p_j, p_k\right]^T$

$$N_i = \frac{1}{2\Delta^{(e)}}(a_i + b_i x + c_i z)$$

$$N_j = \frac{1}{2\Delta^{(e)}}\left(a_j + b_j x + c_j z\right)$$

$$N_k = \frac{1}{2\Delta^{(e)}}\left(a_k + b_k x + c_k z\right)$$

$$\Delta^{(e)} = \frac{1}{2} det \begin{bmatrix} 1 & x_i & z_i \\ 1 & x_j & z_j \\ 1 & x_k & z_k \end{bmatrix}$$

$$a_i = x_j z_k - x_k z_j, \quad b_i = z_j - z_k, \quad c_i = x_k - x_j$$

$$a_j = x_k z_i - x_i z_k, \quad b_j = z_k - z_i, \quad c_j = x_i - x_k$$

$$a_k = x_i z_j - x_j z_i, \quad b_k = z_i - z_j, \quad c_k = x_j - x_i$$

Substituting (3.23) into (3.22), the element equation (3.21) become;

$$A^{(e)}\phi^{(e)} - B^{(e)}\phi^{(e)} = 0$$

where;

$$A^{(e)} = \frac{c^2}{4\Delta^{(e)}} \begin{bmatrix} b_i^2 + c_i^2 & b_i b_j + c_i c_j & b_i b_k + c_i c_k \\ b_i b_j + c_i c_j & b_j^2 + c_j^2 & b_j b_k + c_j c_k \\ b_i b_k + c_i c_k & b_j b_k + c_j c_k & b_k^2 + c_k^2 \end{bmatrix}$$

$$B^{(e)} = \frac{c^2}{4\Delta^{(e)}} \begin{bmatrix} c_i^2 & c_i c_j & c_i c_k \\ c_j c_i & c_j^2 & c_j c_k \\ c_k c_i & c_k c_j & c_k^2 \end{bmatrix}$$

$$\phi^{(e)} = \left[p_i, p_j, p_k\right]^T$$

3.2.6 Convergence Rates

A numerical analyst is always greatly concerned about the accuracy of the numerical solutions. For finite-element-method procedures, the question is "How do the errors decrease when we put nodes closer together?" It can be shown that, with linear elements, errors are of order $0(h^2)$, where h is a measure of the nodal spacing. Quadratic elements give an $0(h^3)$ accuracy; higher orders than two give even better accuracy as the mesh is refined. As we have said, the rate of decrease is a limit value that is achieved only as the h-value gets very small. (The rate of decrease in the errors with quadratic or higher-order shape functions also depends on the integration method used in formulating the system of equations.) Also, a very interesting phenomenon has been observed in studies of the effect of smaller h-values on accuracy-errors may not always decrease uniformly as the spacing is made closer. As a mesh is gradually refined, anomalous behavior can occur. It is frequently the case that nodes are not uniformly spaced in fact, this is one of the major advantages of the finite-element method; we can put nodes closer together where the solution u(x) varies most rapidly to get better accuracy in that sub region. (Curtis and Patrick 2004).

CHAPTER FOUR

RESULTS AND DISCUSSIONS

4.1 Results Analysis

The formulation developed in section 3.2.5 above will be solved using dimensionless cylindrical coordinates, where the $x = rcos\theta, z = rsin\theta$ within the domain $r \in [1,2]$, $\theta \in \left[0, \frac{\pi}{6}\right]$. The acoustic wave equation in cylindrical coordinates (r, θ, t) see equation (3.9), when solved using the initial conditions as given in section 3.2.2, boundary conditions given in section 3.2.3 and on discretising the equation reduces to; $[M]\{p\} + C^2[K]\{p\} = 0$

where K and M are stiffness and mass matrices respectively, $K_e = \int_{\Omega_e} (\nabla N)^T \nabla N d\Omega_e$ and $M_e = \int_{\Omega_e} N^T d\Omega_e$ where Ω_e is the domain of the element and N is the basis function matrix, the exact solution for this problem, using Bessel function of the first kind is as given in equation (3.11) where at $t = 0$. the initial condition for pressure becomes $p(r, \theta, 0) = 0$

To ascertain the quality and correctness of a numerical solution, a comparison with a known solution should be performed. The exact solutions were described in terms of Bessel function of the first kind

The graph below shows the Bessel function of the first kind versus radius.

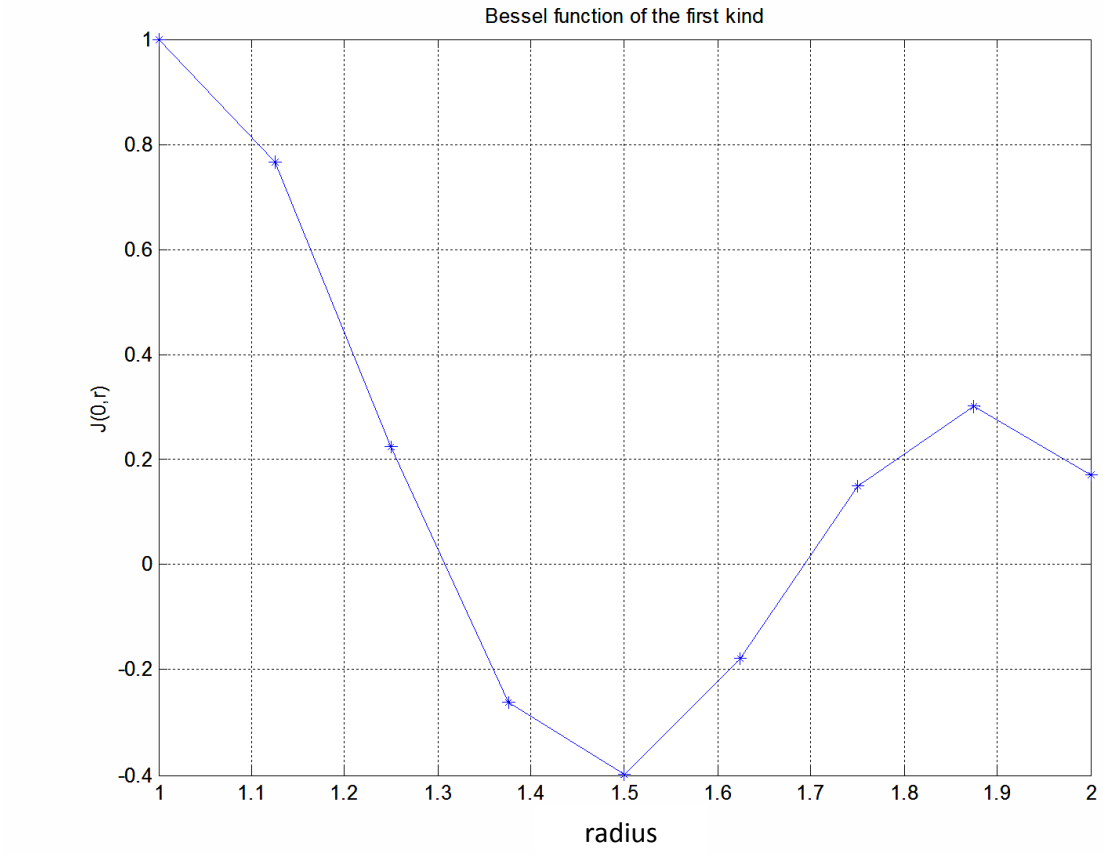

Figure 4.1. Bessel function of the first kind $J_n(r)$ versus radius

Figure 4.1 shows the solutions of wave equation at the nodal points given by the Bessel function of the first kind to the radial part. The Bessel function behaviour looks like oscillating sine or cosine functions, hence periodic.

The boundary conditions applied at the boundaries of the numerical grid are the free surface boundary condition at r =1 and the absorbing boundary condition applied at the edges of the grid at r =2. The solution is based on considering wave motion in the direction normal to the boundary, which in this case is the radial direction over radial angle $\theta \in [0^o, 30^o]$.

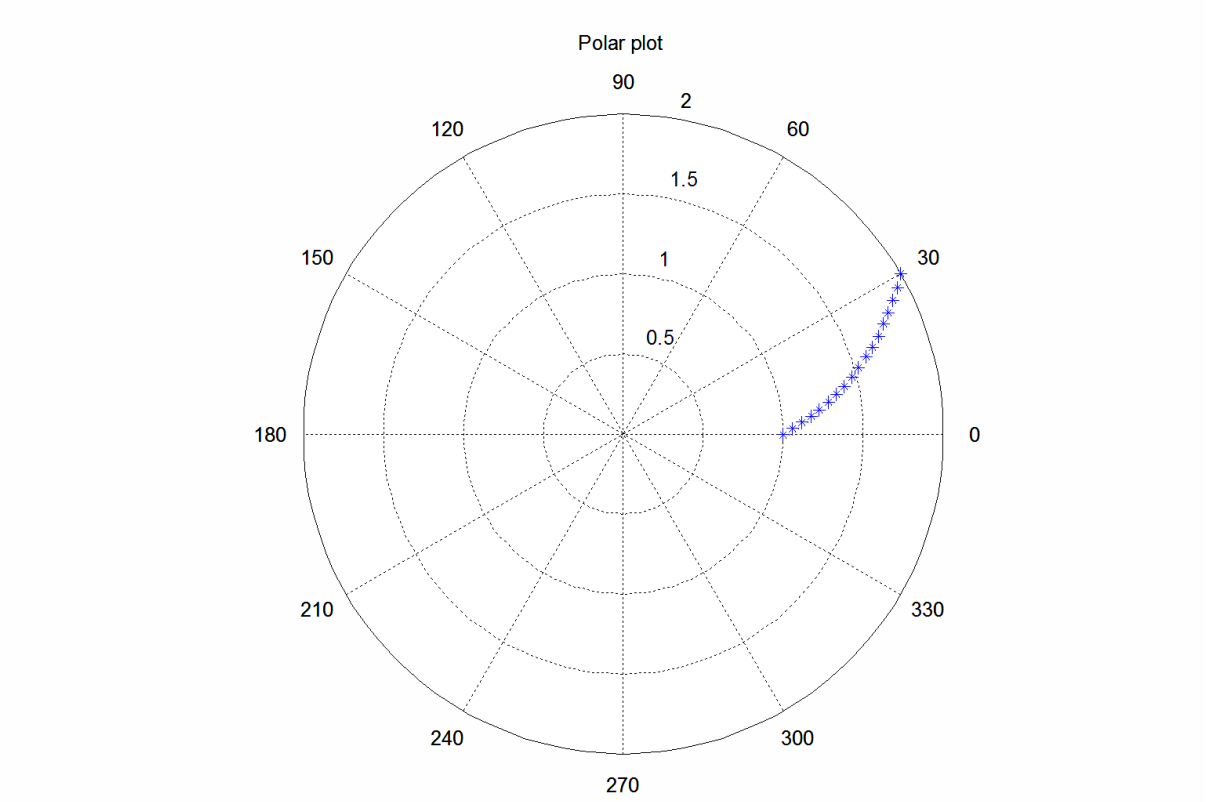

Figure 4.2. The polar plot of the numerical grid and the blue ensterix represents the domain to be discretised to triangular elements.

The solution of the acoustic wave equation was obtained by using the MATLAB code (as given in the appendix) by solving the pressure variable over the domain using the exact solution which was obtained from the Bessel function of the first kind. The boundary conditions for pressure were obtained from the exact solution. For the numerical solution, the domain was discretised using linear triangular elements and the element intervals are as shown in fig 3.5.

Time integration was done using finite difference. Other ordinary differential equation solvers can also be used for instance ode45. The table below illustrates the numerical solution and the exact solution of pressure over the nodal points 1-9 and the absolute error.

Table 1; The Numerical solution and the exact solution of pressure over nodal points 1-9 and the absolute error

NODE	NUMERICAL	EXACT	ABSOLUTE ERROR
1	57.9164	57.9164	0
2	32.6593	38.6481	5.9888
3	0	0	0
4	34.1447	34.1447	0
5	29.7743	30.1721	0.3978
6	0	0	0
7	3.78	3.786	0.006
8	20.3786	18.6147	1.7639
9	0	0	0

The above table shows numerical and exact pressure values for each nodal point from 1-9, over radial angle $\theta \in (0, \frac{\pi}{6})$. It also shows the absolute error of the pressure values for each nodal point. From table 1, it is observed that nodal points 2,5,7 and 8 have shown significant values of absolute error. While at nodal points 1,3,4,6 and 9, the absolute error is zero (0). As seen in Figure 3.4 the nodal points 3,6 and 9 lie along radial angle $\theta = 0$, hence the numerical and exact values of pressure are zero (0).

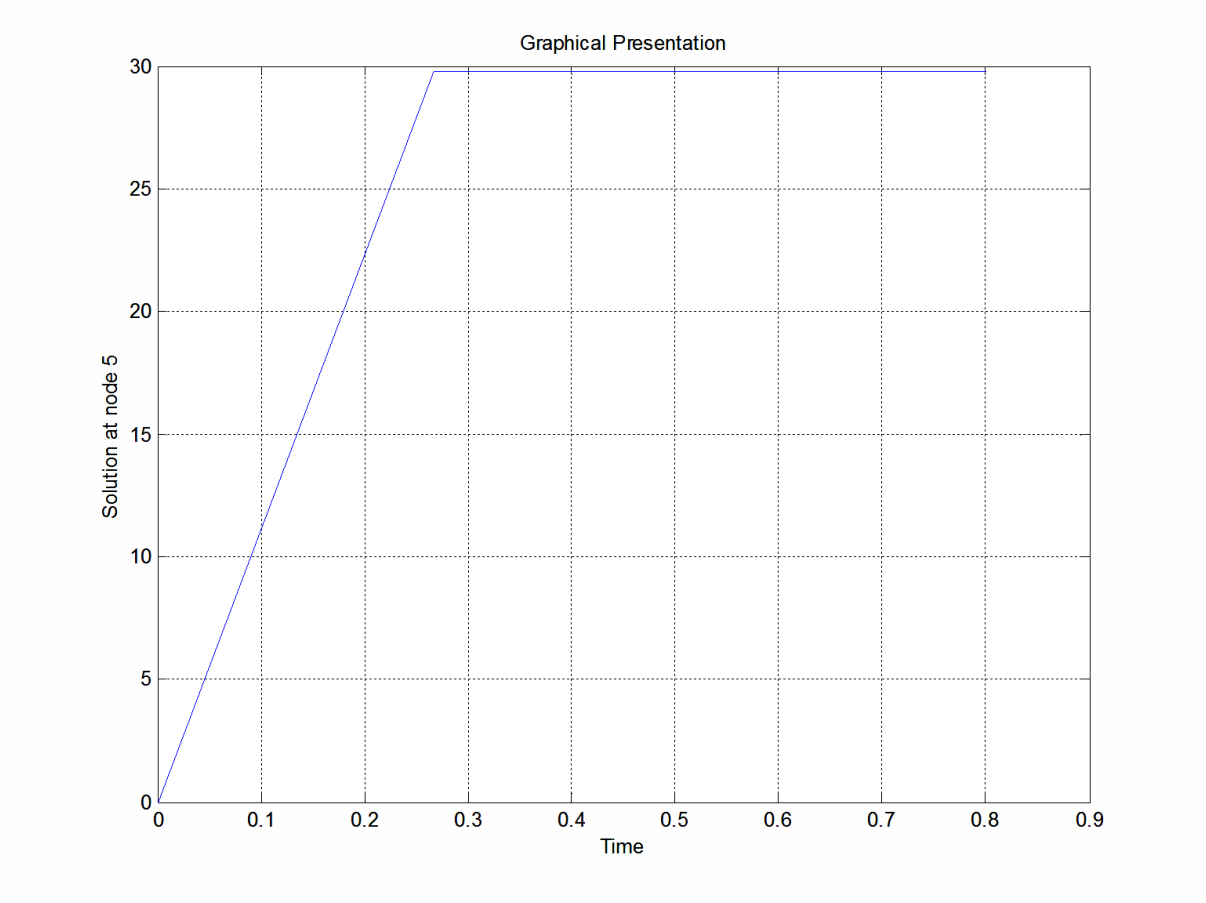

Figure 4.3. Graphical representation of the numerical solution of pressure at nodal point 5 with time

At $t \in (0.2, 0.3)$, the numerical values of pressure are generally obtained for all the nodal points.

A comparison between numerical solution and analytical solution for values of pressure against $r \in [1,2]$ is represented graphically in the figure below.

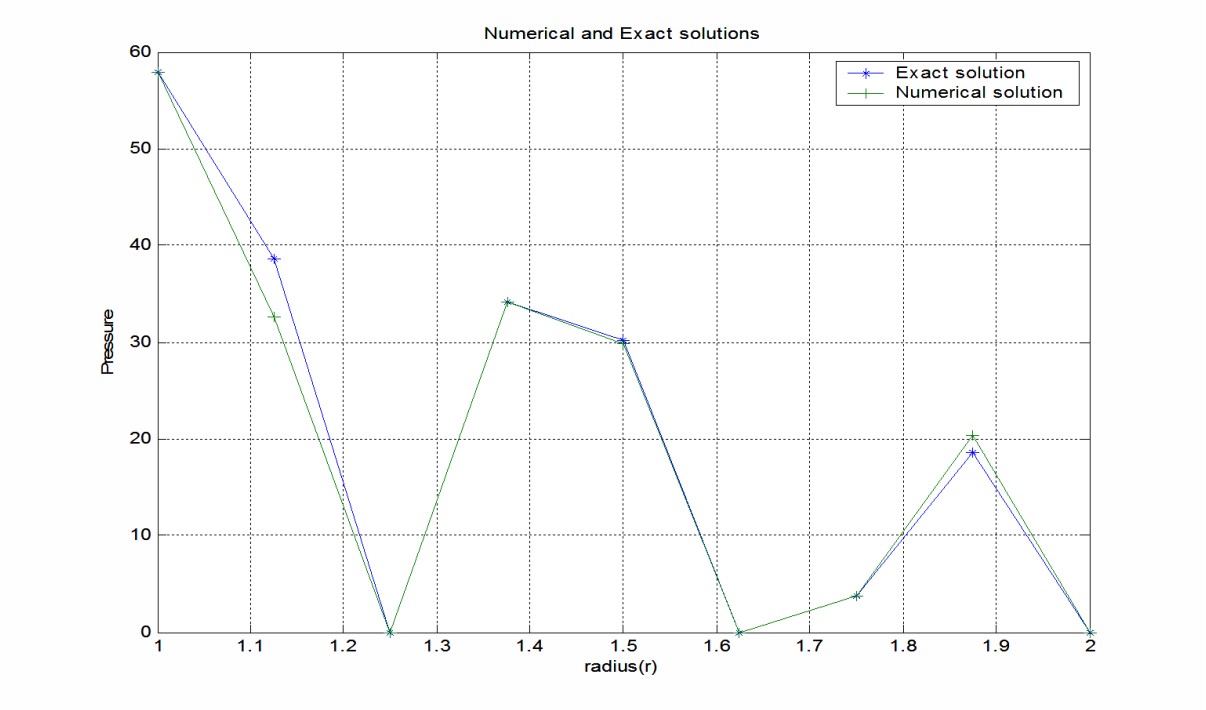

Figure 4.4; Graphical comparison between numerical solution and exact solution

Figure 4.4 shows graphical comparison between numerical solution and exact solution of pressure for each nodal point from 1-9 against the radial direction $r \in (1,2)$, over radial angle $\theta \in (0,\frac{\pi}{6})$. The nodal points at radial angle $\theta = 0$ shows the values of pressure to be zero (0)

A surface response for pressure over radial angle in radians and the radius was also generated as shown in the diagram below.

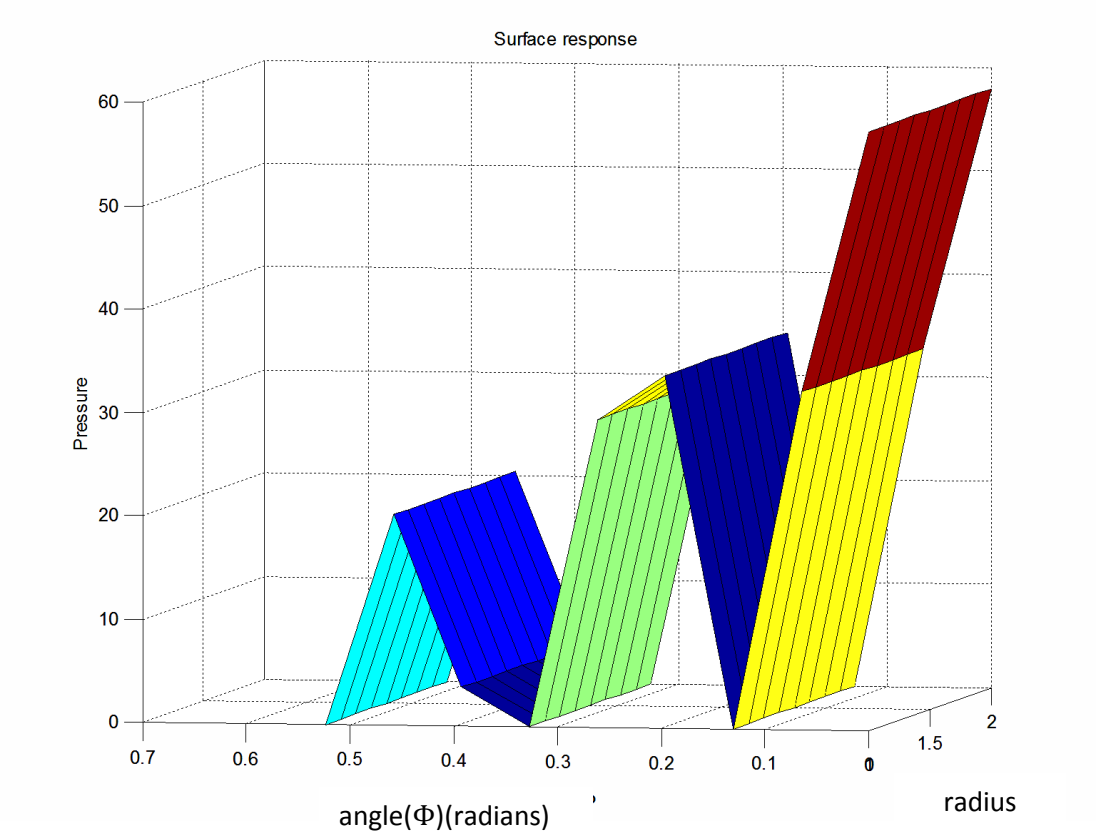

Figure 4.5; surface response showing the values of pressure for each nodal point from 1-9 over radial angle (Φ) in radians and the radius (r).

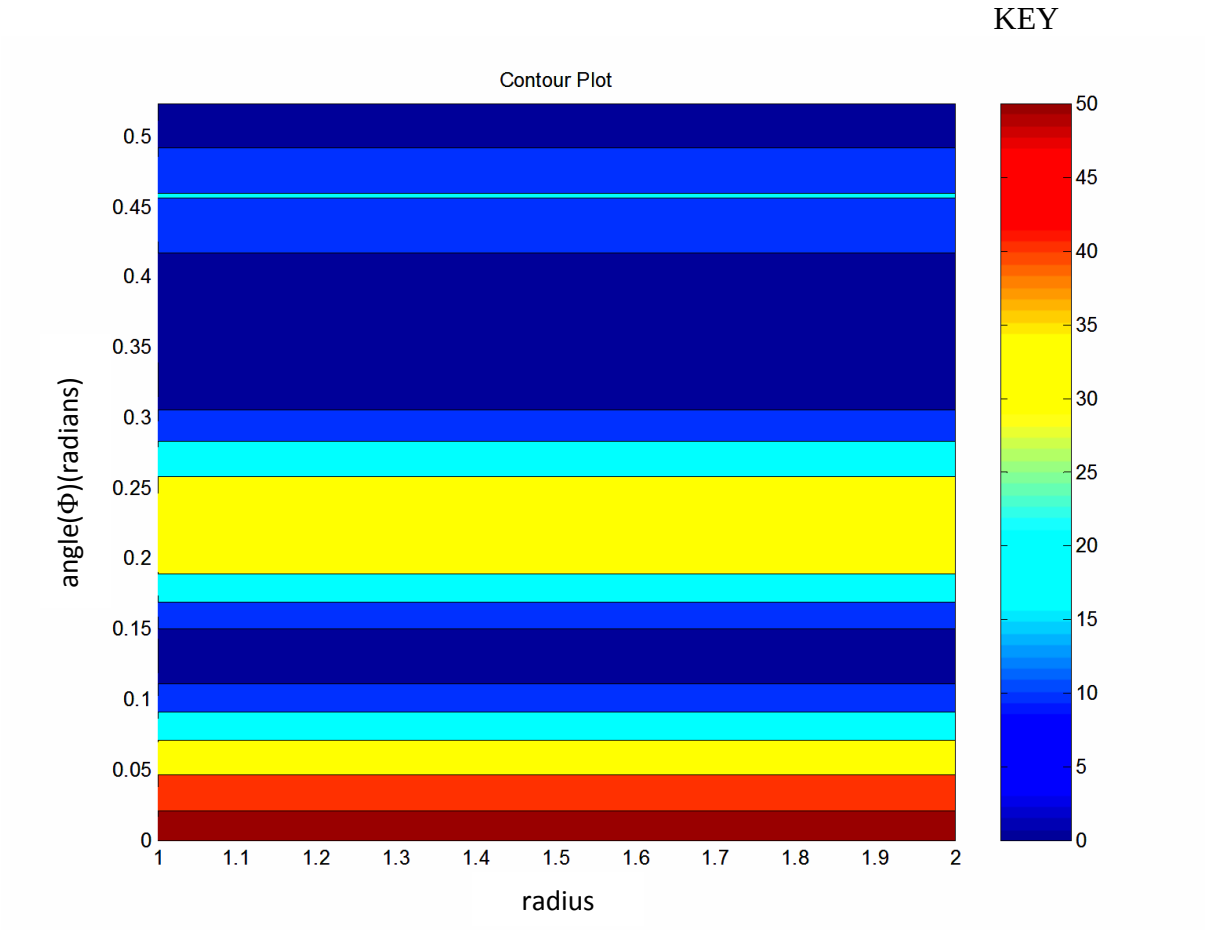

Figure 4.6: contour plot of values of pressure over radial angle (Φ) in radians and the radius. Besides the contour plots sketch is the key to pressure values. The intense red plot signifies the greatest value of pressure.

4.2 Discussion

The analytical solution described in terms of Bessel function of the first kind forms the basis of sufficient accuracy of the numerical solution. Table 1 shows the numerical and exact values of pressure for each nodal point from 1-9 over radial angle $\theta \in (0, \frac{\pi}{6})$. The comparison between the numerical solution and the exact solution shows that the absolute error is zero (0) in nodes 1,3,4,6 and 9. The numerical and exact values of pressure in nodal points 3,6 and 9 are zero (0) hence absolute error is zero (0). These nodal points lie along the radial angle $\theta = 0$ where the pressure values

are generally zero (0). The nodal points 1 and 4 lie at radial angle $= \frac{\pi}{6}$. At these two points the absolute error is zero (0), meaning the numerical solution and the exact solution of pressure at these nodal points is generally the same. This is due to lesser curved boundaries particularly at $r, \theta \in (1, \frac{\pi}{6})$ and at $r, \theta \in \left(1.5, \frac{\pi}{6}\right)$.

At nodal points 2,5,7 and 8 there are significant values of absolute error, meaning the numerical solution and the exact solution of pressure generally differs. At nodal point 2 the absolute error is higher than in nodal point 5,7 and 8 but very minimal in node 7. Refer to figure 3.4. The variations of the numerical values of pressure with the exact values of pressure are due to the increased curved boundaries, which basically decreases as the radius increases.

Errors can be improved by refining the mesh using more triangular elements over the numerical grid or domain, by choosing the time interval of obtaining the numerical and the exact solution. In this research the time interval $t \in (0.2, 0.3)$ was used.

Errors can also be improved by use of higher order elements like the quadratic elements. However, solutions at the curved boundaries are less accurate.

Figure 4.3 shows the graphical representation of the numerical solution of pressure at nodal point 5 over the function time, which means at $t \in [0.2, 0.3]$ the numerical solution is obtained for generally all the nodal points.

Figure 4.4 shows a comparison between numerical solution and exact solution of pressure values against $r \in [1,2]$ over radial angle $\theta \in (0, \frac{\pi}{6})$. The nodal points at radial angle $\theta = 0$ shows the numerical and exact values of pressure to be zero (0). This means there is generally a perfect match between the numerical and exact results.

A surface response for pressure over radial angle in radians(Φ) and the radius was also generated as shown in figure 4.5, which shows that there is an increase in pressure values for each nodal point from 1-9 as the radius increases.

Figure 4.6 shows the contour plots of pressure values over radial angle in radians (Φ) and the radius. Using the given key, the pressure values are generally the greatest at the greatest values of radius.

CHAPTER FIVE

CONCLUSION AND RECOMMENDATIONS

5.1 Conclusion

This thesis has presented the discontinuous Garlerkin time domain numerical method with the use of MATLAB code to solve the acoustic wave equation in 2-D cylindrical coordinates. The method is very useful in study of the pressure effects in wave propagation in fluids. The solution scheme is based on describing the exact solution in terms of Bessel function of the first kind and then developing the numerical solution. From the findings, a comparison between numerical solution and analytical solution for pressure shows that, there is an almost perfect match between the numerical solution and analytical results. This demonstrates that the method can very accurately handle wave propagation in homogenous medium, including propagation on the surface of a cylindrical object. From the findings we can also conclude that, pressure of the wave increases as the radius increases within the same radial angle. The domain was discretised using linear triangular elements, however the solutions at the curved boundaries are slightly less accurate from the values of absolute errors obtained. The errors can be improved by refining the triangular mesh by using more triangular elements over the numerical grid or domain, carefully choosing the time variable and by use of higher order elements i.e quadratic elements. However, the only problem with small elements is that they can lead to small time step which can increase the overall computational cost in terms of time. The main advantage of DGTM over other numerical methods as a finite element method is that it can be adopted to problems of complex geometries (boundaries and interfaces). It also has high order accuracy and stability, however it is costly in terms of time, it requires a considerable amount of memory and computational costs.

5.2 Recommendations

More work still remains undone in the field of acoustic wave propagation and in the implementation of the solution models. Following the results of this work, we would recommend further research on the following areas;

1) To solve the 2-D acoustic wave equation using discontinuous Galerkin time domain method on more refined meshes on non-uniform boundaries using cylindrical coordinates.
2) To solve the 3-D acoustic wave equation using DGTM method on cylindrical coordinates and compare with the analytical solution.
3) To solve the non-linear acoustic wave equation on heterogeneous medium using DGTM method, which is a finite element method.

REFERENCES

Ahmad Z. (2000) *The two dimensional Numerical modelling of acoustic wave propagation in shallow water*, Joondalup, Australia

Arfken G and Weber H.(2001) *Mathematical Methods for Physicists*. Academia Press

Arnord D, Brezzi F, Cockburn B and Marini L.D. (2001) A Unified Analysis of Discontinuous Galerkin Methods for Elliptic Problems, *SIAM Journal:* pp.231-354

Atangana A (2013) On the solution of an acoustic wave equation with variable-order derivative loss operator; Advances in Difference Equations, *Springer Journal* 167

Atkins, H and Shu C,W. (1998*)* Quadrature-free implementation of the Discontinuous Galerkin method for hyperbolic equations; *AIAA Journal* 36 pp 775-782

Benjamin D (2015) *A study into Discontinuous Galerkin Method for the second order wave Equation*, Naval Postgraduate School, Moterey,

Celiber F and Cockburn B. (2007) *Mathematics of Computation*, Berlin

Cockburn B, Karniadakis G and Shu C.(2000)Discontinuous Galerkin Methods; Theory, Computation and Applications, *lecture notes in computational science and engineering Volume 11*, Berlin

Cockburn B and Shu C, (1998) The local Discontinuous Galerkin Finite Element Method for Convection-Diffusion Systems, *SIAM Journal*, Berlin : pp.56-98

Curtis G and Patrick W. (2004) *Applied Numerical Analysis* 7th edition, Pearson Addison Wesley, U.S.A.

Darrell W and Juan C (2017) *The Finite Element Method Basic Concepts and Applications with MATLAB, MAPLE and COMSOL, 3th edition,* CRC Press Boca Raton London Newyork,

David K and Dan K (1990) Acoustic wave propagation in 2-D cylindrical coordinates, *Geophysics J.Int,*103 : pp.577-587

Erickson K and Johnson C. (1991) Element Methods for Parabolic Problems, S*IAM Journal* :vol 32 No 6 pp. 1750-1763

Eskilsson C and Sherwin S. (2005) Discontinous Galerkin Spectral/hp element modelling of dispersive shallow water systems, *Journal of Scientific Computing* 22-23 pp 269-288

Frank F and David T, (2015) *Fundamentals of Sound and Vibration 2nd edition* , CRC Press Boca Raton London Newyork,

Grote M and Schneebeli A, (2006) Discontinuous Galerkin Finite Element Method for the Wave Equation, *SIAM Journal* : pp. 81-112

Herrin D. (2012) *The Wave equation and it's solution in Gases and Liquids*, Department of Mechanical Enginerring, University of Kentucky, Lexington

Hesthaven. J and Warbuton.T, (2007) *Nodal Discontinous Galerkin Methods; Algorithms, Ana*lysis *and Applications* , Springer

Houston P, Jensen M and Suli E. (2002) *hp-Discontinuous Galerkin Finite Element Methods with Least Squares Stabilisation,* J.Sci.Computation 17(1-4),: pp,3-25

Jain M.K, (1986) *Numerical Solution of Differential Equations 2nd Edition,* wiley Eastern,New Delhi

Jenssen F, William A, Michael B, Henrick S. (2011) *Computational Ocean Acoustics* 2nd edition, Springer-Verlag Newyork,

Kaser M, and Dumbser M, (2006) An arbitrary high-order discontinuous Galerkin Method for elastic waves on unstructured meshes-I, The two dimensional Isotropic case with external source terms, *Geophysical Journal International* 166; pp 224-242

Klockner A, Warburton T, Bridge J and Hesthaven J, (2009) *Nodal discontinuous Galerkin methods on graphics processors* Journal of Computational Physics volume 228, pp 7863-7882

Margrave G, (2000) New Seismic Modelling facilities in Matlab, *CREWES Report* 12,

Matt A. McDonald, Michael P. Lamoureux, Gary F. Margrave, (2012) Galerkin Mettods for numerical solutions of acoustic, elastic and viscoelastic wave equations. *CREWES Research report* – volume 24 :

Mohamed I, Othman A, Mahamed G and Roushid M, (2011), Analytical solution for Acoustic waves propagation in fluids, *world Journal of mechanics*, department of Physics faculty of science, Minia University, Minia, Egypt, 1, pp.243- 246

Ober C, Smith T, Collis S, Overfelt J and Schwaiger H, (2010) *Elastic wave propagation in variable media using a discontinuous Galerkin method*, Conference paper, Technical report, Sandia National Laboratories

Pierce A, Acoustics, (2019) *An Introduction to its physical principles and Applications 3rd edition*, Springer Nature Switzerland AG

Powers M, (2017) *Lecture notes on Mathematical Methods II*, Department of Aerospace and Mechanical Engineering, Notre Dame, Indiana, USA

Prem K. Kythe, Pratap Puri, and Michael R. Schaferkotter, (2017) *Partial differential equations and boundary value problems with mathematica 2nd edition*, Chapman $ Hall/CRC, Florida.

Renzo A, (2016) Validation of Discontious Galerkin Implementation of the Time-Domain Linearized Navier-stokes equations for Aeroacoustics, *Aerospace 3,7; doi 10.3390/aerospace3010007*

Reed W.H and Hill T.R, (1973) *Triangular Mesh Methods for neutron transport equation* Los Alamos

Sandip M, (2016) *Numerical Methods for Partial Differential equations- Finite Difference and Finite Volume Methods*, Elsevier, Oxford

Shabazi K, Fischer P and Ethier C, A high-order discontinuous Galerkin method for unsteady incompressible Navier-Stokes equations, *Journal of Computational Physics* 222, (2007) pp 391-407

Simonaho S, Lhivaara T and Huttunen T, (2012) Modelling of acoustic wave propagation in time-domain using the discontinuous Galerkin method- a comparison with measurements applied acoustics, volume 73(2); pp 173-183

Symes W, Mathematics of Seismic Imaging (2003) *Computational Geosciences volume 13* pp 363-371

Tetyana V,Susan E and Oksana P. (2005) Operator Upscalling for the acoustic wave equation, SIAM Journal, volume 4 No. 4 pp1305-1338

Timo L, (2010) *Discontinous Galerkin method for Time-Domain wave problems*, University of Eastern Finland, Kuopio

Wang S, (2017) *Finite difference and Discontinous Galerkin Methods for wave equations,* Acta universitatis , Uppsala

Wang X, Symes W and Warburton T, (2010*)* Comparison of discontinuous Galerkin and Finite difference methods for time domain acoustics, *Technical programs* volume 29, pp 3060-3065

Youzwishen C and Margrave G, (1999) Finite difference modelling of acoustic waves in Matlab, *CREWES Research Report* 11

Zhebel E, Minisini S, Kononov A and Mulder W. (2013) Performance and scalability of Finite difference and Finite element wave propagation Modelling on Intel's Xeon phi, *Technical programs* pp 3386-3390.

APPENDICES

Appendix I
MATLAB CODE FOR ANALYTICAL AND NUMERICAL SOLUTION TO ACOUSTIC WAVE EQUATION.

function acoustic

```
% To solve p_tt=p_rr+(p_r/r)+(p_phi,phi)/r^2
% 0=<phi=<pi/6 radians,1=<r=<2,0=<t=<1
% Using linear triangular elements and Finite
% difference method for time integration
% ######################################################
% control parameters
% ######################################################
nel=8;
nnel=3;
ndof=1;
nnode=9;
sdof=nnode*ndof;
dt=0.267;
stime=0;
deltaphi=pi/12;
deltar=0.5;
ftime=1;
nt=fix((ftime-stime)/dt);
% ######################################################
% nodal coordinate values / Transformed
% ######################################################
% gcoord(i,j)=r*cos(phi);gcoord(i,j+1)=r*sin(phi)
gcoord(1,1)=0.8660;     gcoord(1,2)=0.5;
gcoord(2,1)=0.9659;     gcoord(2,2)=0.2588;
gcoord(3,1)=1;          gcoord(3,2)=0;
gcoord(4,1)=1.2990;     gcoord(4,2)=0.75;
gcoord(5,1)=1.4672;     gcoord(5,2)=0.3119;
gcoord(6,1)=1.5;        gcoord(6,2)=0;
gcoord(7,1)=1.7321;     gcoord(7,2)=1;
gcoord(8,1)=1.9319;     gcoord(8,2)=0.5176;
gcoord(9,1)=2;          gcoord(9,2)=0;
% ######################################################
% nodal connectivity
% ######################################################
nodes(1,1)=1;nodes(1,2)=2;nodes(1,3)=5;
nodes(2,1)=2;nodes(2,2)=3;nodes(2,3)=6;
nodes(3,1)=1;nodes(3,2)=5;nodes(3,3)=4;
nodes(4,1)=2;nodes(4,2)=6;nodes(4,3)=5;
nodes(5,1)=4;nodes(5,2)=5;nodes(5,3)=8;
nodes(6,1)=5;nodes(6,2)=6;nodes(6,3)=9;
nodes(7,1)=4;nodes(7,2)=8;nodes(7,3)=7;
nodes(8,1)=5;nodes(8,2)=9;nodes(8,3)=8;
% ######################################################
% boundary conditions
```

```
% ######################################################
bcdof(1)=1;
bcval(1)=57.9164;
bcdof(2)=4;
bcval(2)=34.1447;
bcdof(3)=7;
bcval(3)=3.78;
bcdof(4)=3;
bcval(4)=0;
bcdof(5)=6;
bcval(5)=0;
bcdof(6)=9;
bcval(6)=0;
% ######################################################
% initialization
% ######################################################
ff=zeros(sdof,1);
fsol=zeros(sdof,1);
kk=zeros(sdof,sdof);
mm=zeros(sdof,sdof);
index=zeros(nnel*ndof,1);
% ######################################################
% computation and assembly
% ######################################################
for iel=1:nel
   nd(1)=nodes(iel,1);
   nd(2)=nodes(iel,2);
   nd(3)=nodes(iel,3);
   x1=gcoord(nd(1),1);y1=gcoord(nd(1),2);
   x2=gcoord(nd(2),1);y2=gcoord(nd(2),2);
   x3=gcoord(nd(3),1);y3=gcoord(nd(3),2);
   index=feeldof(nd,nnel,ndof);
   k=felp2dt3(x1,y1,x2,y2,x3,y3);
   m=felpt2t3(x1,y1,x2,y2,x3,y3);
   kk=feasmblk(kk,k,index);
   mm=feasmblm(mm,m,index);
end
%#####################################################################
% Time integration using Finite difference and Solution/ output
%#####################################################################
%
p(r,phi,t)=besselj(0,mu*r/c)*[Acos(mu*t)+Bsin(mu*t)]*[Ccos(k*phi)+Dsin(k*phi)]
% Exact general solution
for in=1:sdof
   fsol(in)=0;
end
sol(1,1)=fsol(5);
for it=1:nt
    M=(((dt^2)*inv(mm)*kk)-2*eye(9));
   [M,ff]=feaplyc2(M,ff,bcdof,bcval);
```

```
   fsol=M\ff;
   sol(1,it+1)=fsol(5);
end
%-------------------------------------------------
% Analytical solution
%-------------------------------------------------
for i=1:nnode
   r=gcoord(i,1);phi=gcoord(i,2);t=1;
   esol(i)=100*(besselj(0,r)*sin(pi*t/4)*sin(3*phi));
end
num=1:1:sdof;
Results=[num' fsol esol' abs(fsol-esol')]
figure(1)
time=0:dt:nt*dt;
plot(time,sol(1,:))
grid
xlabel('Time'),ylabel('Solution at node 5')
title('Graphical Presentation')
figure(2)
[R,PHI]=meshgrid(1:1/8:2,0:pi/(8*6):pi/6);
z=fsol;
Z=[z z z z z z z z];
contourf(R,PHI,Z),colorbar
grid
xlabel('radius(r)'),ylabel('angle(\phi)')
title('Contour Plot')
figure(3)
r=[1:1/17:2];
phi=[0:pi/(17*6):pi/6];
polar(phi,r,'*')
grid
title('Polar plot')
% ########################################################
% M-files   used in the main program
% ########################################################
%[M]*p_tt=[K]*p=0
%########################################################
function [m]=felpt2t3(x1,y1,x2,y2,x3,y3)
A=0.5*(x2*y3+x1*y2+x3*y1-x2*y1-x1*y3-x3*y2);
m=(A/12)*[2 1 1;1 2 1;1 1 2];
%---------------------------------------------------------
function [k]=felp2dt3(x1,y1,x2,y2,x3,y3)
% Element matrix  for 2D using 3-node linear tringular element
A=0.5*(x2*y3+x1*y2+x3*y1-x2*y1-x1*y3-x3*y2);
rc=(x1+x2+x3)/3;
k(1,1)=(rc*(x3-x2)*(x3-x2)+(y2-y3)*(y2-y3)/rc)/(4*A);
k(1,2)=(rc*(x3-x2)*(x1-x3)+(y2-y3)*(y3-y1)/rc)/(4*A);
k(1,3)=(rc*(x3-x2)*(x2-x1)+(y2-y3)*(y1-y2)/rc)/(4*A);
k(2,1)=k(1,2);
k(2,2)=(rc*(x1-x3)*(x1-x3)+(y3-y1)*(y3-y1)/rc)/(4*A);
```

```
k(2,3)=(rc*(x1-x3)*(x2-x1)+(y3-y1)*(y1-y2)/rc)/(4*A);
k(3,1)=k(1,3);
k(3,2)=k(2,3);
k(3,3)=(rc*(x2-x1)*(x2-x1)+(y1-y2)*(y1-y2)/rc)/(4*A);
%-----------------------------------------------
function [kk]=feasmblk(kk,k,index)
% Assembly of element matrices
edof=length(index);
for i=1:edof
   ii=index(i);
   for j=1:edof
      jj=index(j);
      kk(ii,jj)=kk(ii,jj)+k(i,j);
   end
end
%-----------------------------------------------
function [mm]=feasmblm(mm,m,index)
% Assembly of element matrices-TRANSIENT TERM
edof=length(index);
for i=1:edof
   ii=index(i);
   for j=1:edof
      jj=index(j);
      mm(ii,jj)=mm(ii,jj)+m(i,j);
   end
end
%-----------------------------------------------
function [index]=feeldof(nd,nnel,ndof)
% System dofs
edof=nnel*ndof;
count=0;
for i=1:nnel
   start=(nd(i)-1)*ndof;
   for j=1:ndof
      count=count+1;
      index(count)=start+j;
   end
end
%-------------------------------------------------
function[M,ff]=feaplyc2(M,ff,bcdof,bcval)
% boundary conditions
n=length(bcdof);
sdof=size(M);
for i=1:n
   c=bcdof(i);
   for j=1:sdof
      M(c,j)=0;
   end
   M(c,c)=1;
   ff(c)=bcval(i); end
```

Appendix II: Similarity Index/Anti-Plagiarism Report

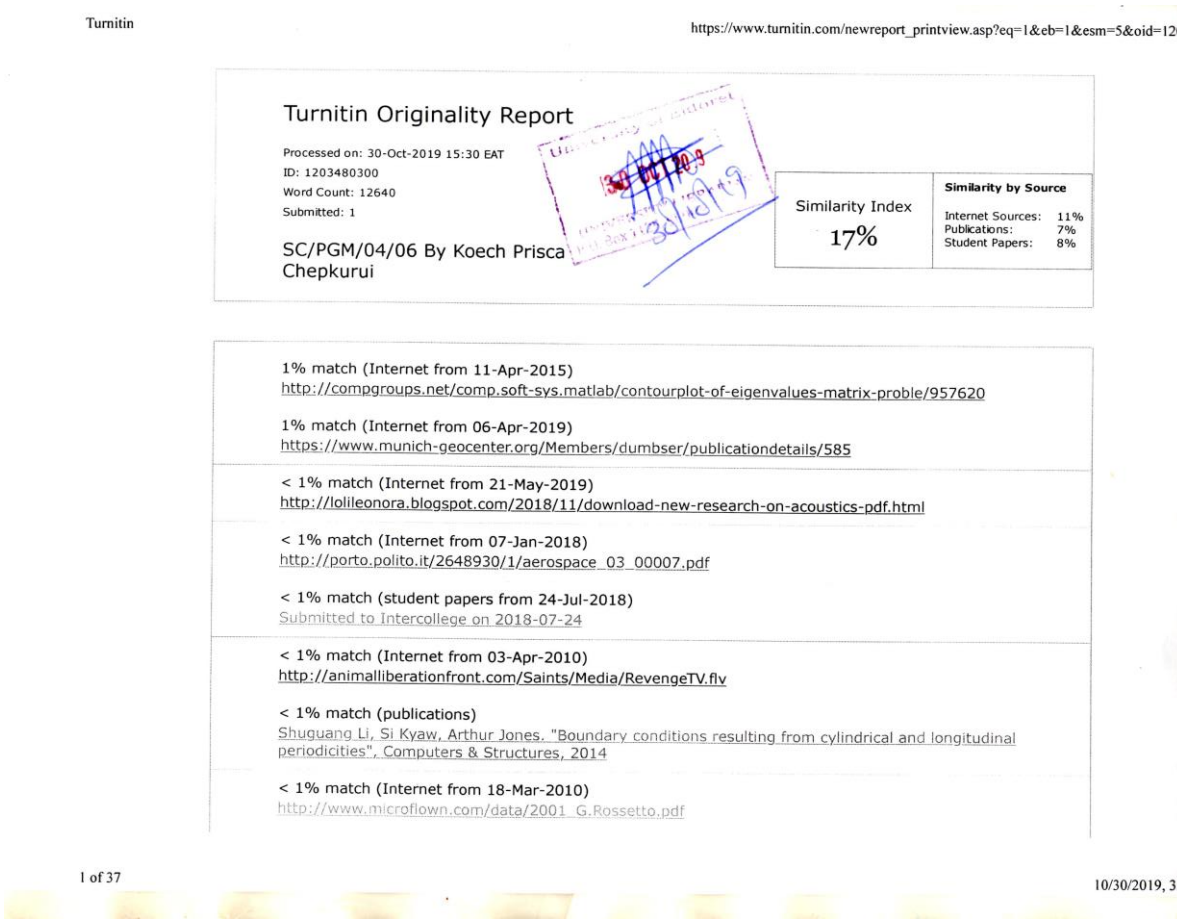

Turnitin https://www.turnitin.com/newreport_printview.asp?eq=1&eb=1&esm=5&oid=12

Turnitin Originality Report

Processed on: 30-Oct-2019 15:30 EAT
ID: 1203480300
Word Count: 12640
Submitted: 1

SC/PGM/04/06 By Koech Prisca Chepkurui

Similarity Index	Similarity by Source	
17%	Internet Sources:	11%
	Publications:	7%
	Student Papers:	8%

1% match (Internet from 11-Apr-2015)
http://compgroups.net/comp.soft-sys.matlab/contourplot-of-eigenvalues-matrix-proble/957620

1% match (Internet from 06-Apr-2019)
https://www.munich-geocenter.org/Members/dumbser/publicationdetails/585

< 1% match (Internet from 21-May-2019)
http://lolileonora.blogspot.com/2018/11/download-new-research-on-acoustics-pdf.html

< 1% match (Internet from 07-Jan-2018)
http://porto.polito.it/2648930/1/aerospace_03_00007.pdf

< 1% match (student papers from 24-Jul-2018)
Submitted to Intercollege on 2018-07-24

< 1% match (Internet from 03-Apr-2010)
http://animalliberationfront.com/Saints/Media/RevengeTV.flv

< 1% match (publications)
Shuguang Li, Si Kyaw, Arthur Jones. "Boundary conditions resulting from cylindrical and longitudinal periodicities", Computers & Structures, 2014

< 1% match (Internet from 18-Mar-2010)
http://www.microflown.com/data/2001_G.Rossetto.pdf

1 of 37 10/30/2019, 3